

Solvation of electronically excited I_2^-

P. E. Maslen, J. M. Papanikolas, J. Faeder, R. Parson, and S. V. O'Neil

Joint Institute for Laboratory Astrophysics and Department of Chemistry and Biochemistry, University of Colorado and National Institute of Standards and Technology, Boulder, Colorado 80309-0440

(Received 2 May 1994; accepted 23 June 1994)

The interaction potentials between the six lowest electronic states of I_2^- and an arbitrary discrete charge distribution are calculated approximately using a one-electron model. The model potentials are much easier to calculate than *ab initio* potentials, with the cost of a single energy point scaling linearly with the number of solvent molecules, enabling relatively large systems to be studied. Application of the model to simulation of electronically excited I_2^- in liquids and CO_2 clusters is discussed. In a preliminary application, solvent effects are approximated by a uniform electric field. If electronically excited (${}^2\Pi_{g,1/2}$) I_2^- undergoes dissociation in the presence of a strong electric field, the negative charge localizes so as to minimize the total potential energy. However, in a weak field the negative charge localizes in the opposite direction, maximizing the potential energy. Based on a study of the field-dependent potential surfaces, a solvent-transfer mechanism is proposed for the electronic relaxation of ${}^2\Pi_{g,1/2}I_2^-$, in contrast to the conventional view of relaxation via electron transfer.

I. INTRODUCTION

I_2^- exhibits a strong absorption spectrum in the 700–900 nm region, corresponding to an electronic excitation from the bound ${}^2\Sigma_{u,1/2}^+$ state to the repulsive ${}^2\Pi_{g,1/2}$ state.¹ In view of the repulsive shape of the excited state potential, one might expect that recombination of excited I_2^- in a solvent would occur slowly, if at all. However, photoexcitation experiments on I_2^- and I_3^- in CO_2 clusters^{2–5} and liquids^{6–11} have detected rapid, coherent relaxation of I_2^- to the ground electronic state. This has prompted a spate of theoretical investigations,^{5,12–16} with the proposed mechanisms hinging on the strong Coulombic interaction between the dihalide or trihalide ion (the solute) and the cluster or liquid (collectively labeled as the solvent). In spite of these studies, the relaxation mechanisms, especially the pathways for electronic relaxation, have yet to be determined conclusively.

A major obstacle to the theoretical investigation of solvated dihalides and trihalides is the determination of the solvent \leftrightarrow solute interaction potential. Considerable progress has been made, based on the premise that the interaction potential is dominated by the classical Coulombic interaction of the charge distributions of the solvent and solute. Early models of solvated I_2^- , Br_2^- , and I_3^- assumed that the charge distribution of the solute ion depended only on the solute geometry,^{12–24} while subsequent models included the distortion of the solute charge distribution by the solvent.^{5,16,17}

The early models predicted that the excess negative charge of the solute is responsible for a fivefold increase in the vibrational relaxation rate compared to the corresponding neutral species, and distortion effects were later found to greatly accelerate the initial vibrational relaxation near the top of the vibrational well. However, it is difficult to draw a direct comparison between theory and experiment, because the simulations were restricted to vibrational relaxation on

the ground electronic state, whereas the experimental results depend on both electronic and vibrational relaxation. Furthermore, the only study to have treated the distortion effects in an entirely self-consistent manner approximated the solvent by a continuum model,¹⁶ which is inapplicable to experimental studies of I_2^- surrounded by less than one solvation shell of CO_2 molecules.

In order to make a rigorous comparison of theory and experiment, the simulations should be extended to include electronic relaxation of the photoexcited solute. This requires not only the solvent \leftrightarrow solute interaction potentials for all states participating in the electronic relaxation, but also the rate of nonradiative electronic transitions. This paper focuses on the construction of simple but qualitatively correct interaction potentials for all relevant electronic states. The distortion of the dihalide ion by the solvent is included, and an explicit form is given for the matrix elements which determine the nonradiative electronic surface hopping probability. We shall consider I_2^- in a cluster of 1 to 22 CO_2 molecules, since this system has been the subject of extensive experimental investigation,^{4,5} though the model to be described can be extended to many other systems.

I_2^- has six low lying potential energy surfaces, each of which could conceivably be involved in the photodissociation dynamics, so an adequate model must encompass all six. While experimentally derived¹⁸ potential energy surfaces exist for the six lowest states of isolated I_2^- , determination of the $I_2^- \leftrightarrow$ solvent potential from experiment is hampered by the broad, unresolved nature of the electronic and vibrational spectra. Because clusters have many degrees of freedom, theoretical determination of the potential energy surfaces for $I_2^-(CO_2)_n$ is a major task and approximations must be made if the potential energy and the forces on each molecule are to be evaluated at each time step in a molecular dynamics simulation.

A common approach is to approximate the potential energy as a sum of pairwise interactions. This is valid for the leading charge-quadrupole term in the $I_2^-(CO_2)_n$ interaction potential and for the bonding between the iodine atoms. However, considering the parallel (axial) polarization energy of I_2^- with polarizability α_{zz} in the net electric field \vec{F} produced by all the CO_2 molecules,

$$\vec{F} = \sum_{i=1}^n \vec{F}_i,$$

$$V = \frac{1}{2} \alpha_{zz} F_z^2,$$

one finds that the polarization energy is composed of two-body terms involving I_2^- and one CO_2 , and three-body terms involving I_2^- and two CO_2 molecules,

$$V = \frac{1}{2} \alpha_{zz} \sum_{i=1}^n F_{zi}^2 + \frac{1}{2} \alpha_{zz} \sum_{i \neq j}^n F_{zi} F_{zj}.$$

For a model system where all the F_{zi} are equal, the three-body term is approximately n times larger than the two-body term. This is merely a demonstration of the well-known fact that electrostatic interactions between permanent multipole moments are pairwise additive whereas those involving induced moments are not. Internally contracted multireference configuration interaction (MRCI) calculations¹⁹ with singles and doubles excitations^{20,21} using effective core potentials and very small sp basis sets,²² show that the ground electronic state of I_2^- has $\alpha_{zz} = 200$ a.u. at equilibrium (6 Bohr) and $\alpha_{zz} = 5000$ a.u. at a bond length of 10 Bohr. Owing to this enormous polarizability, it is difficult to justify the neglect of many-body effects in a study of $I_2^-(CO_2)_n$. Indeed, expressing the polarizability as a perturbation expansion over all electronic states of isolated ($D_{\infty,h}$) I_2^- ,²³

$$\alpha_{zz} = -2 \sum_{k \neq 0}^{\infty} \frac{\mu_{zz0,k}^2}{E_0 - E_k} \quad (1)$$

it is apparent that $\alpha_{zz} \rightarrow \infty$ as $R \rightarrow \infty$ for the ground (${}^2\Sigma_{u,1/2}^+$) state since the ${}^2\Sigma_{u,1/2}^+$ and ${}^2\Pi_{g,1/2}$ electronic states become degenerate as $R \rightarrow \infty$ [Fig. 1(a)] while the corresponding transition dipole moment $\mu_{zz}({}^2\Sigma_{u,1/2}^+, {}^2\Pi_{g,1/2}) \rightarrow -R/2$ as $R \rightarrow \infty$.²⁴ This reflects the fact that, for a sufficiently large bond length, an infinitesimal field will alter the I_2^- charge distribution from completely delocalized ($I^{-1/2}-I^{-1/2}$) to completely localized ($I-I^-$ or I^-I). Neither a strictly localized nor a strictly delocalized description is adequate for the range of bond lengths from equilibrium to dissociation.

The importance of the solvent-solute interaction potential has been encountered in a study of $Br_2^-(CO_2)_n$ by Perera and Amar.¹² They chose the negative charge on each Br atom to be an empirical function of the Br_2^- bond length, independent of the positions of the CO_2 molecules, and treated the $Br_2^- \leftrightarrow CO_2$ interaction potential as a Coulombic interaction between the point charges on the Br atoms and the permanent and induced multipoles of the CO_2 molecules. A similar

approach was adopted by Benjamin *et al.*¹³ in a study of I_3^- in ethanol, and by Papanikolas¹⁷ in a study of $I_2^-(CO_2)_n$. However, Perera and Amar have noted that the empirical charge switching function is unsatisfactory,²⁵ and Papanikolas found that molecular dynamics simulations of $I_2^-(CO_2)_n$ became trapped in a local minimum, with all the CO_2 molecules surrounding a single I^- ion. A serious shortcoming of these models is that they predict the polarizability of the dihalide ion to be either zero or equal to the atomic polarizability of the neutral halogen atoms, whereas the (adiabatic) polarizability actually diverges to infinity as the bond is stretched [Eq. (1)]. Papanikolas *et al.* subsequently improved the agreement between experiment and simulation by including the CO_2 coordinates in a semiempirical charge switching function.^{5,17} However, even for the ground electronic state of I_2^- , it is exceedingly difficult to fit a multidimensional charge switching function, and a less empirical approach is necessary if all six states are to be considered. The empirical approach also provides no information about electronic properties other than the energy, such as the nonradiative electronic transition rates.

For weakly interacting molecules, an alternative to the pair-potential approach is to calculate the interaction potential from the multipoles and polarizabilities of the isolated fragments. This would require the polarizability of each of the six states of I_2^- as a function of bond length in the range probed by experiment (equilibrium to dissociation³). However, owing to the infinite polarizability of $D_{\infty,h}I_2^-$ at long bond lengths, such a procedure would break down in the dissociative limit. The instability arises because several of the electronic states of I_2^- become degenerate at long bond lengths whereas polarizabilities are based upon nondegenerate perturbation theory [Eq. (1)]. This deficiency can be overcome via degenerate perturbation theory, using a 6×6 Hamiltonian matrix to cope with near degeneracies among the six low lying states of I_2^- . Our approach uses this model Hamiltonian, described in Secs. II and IV, to extract the charge switching behavior from the experimentally derived potential energy surfaces for isolated I_2^- . It is essentially an extension of the model used by Gertner and Hynes¹⁶ who implicitly solved for the ground state eigenvalue of a two state Hamiltonian which treats degeneracies between the ground state and the first excited electronic state of the same symmetry. While Gertner and Hynes focused on vibrational relaxation on the ground electronic state and used a continuum model for the solvent, we are interested in both vibrational and electronic relaxation. We also choose to model the molecular composition of the solvent explicitly, rather than using a continuum model, so the implementation of the two schemes differs considerably.

Although our principal goal is to model I_2^- surrounded by explicit solvent molecules, I_2^- in a uniform electric field is also discussed because the Hamiltonian matrix elements are considerably simpler than for more realistic interaction potentials. One may ask whether the uniform field would provide a reasonable model of solvation effects. At first sight it appears to be a poor model, since internal electric fields in clusters stem from localized charge distributions and more closely resemble Coulombic fields than uniform fields. How-

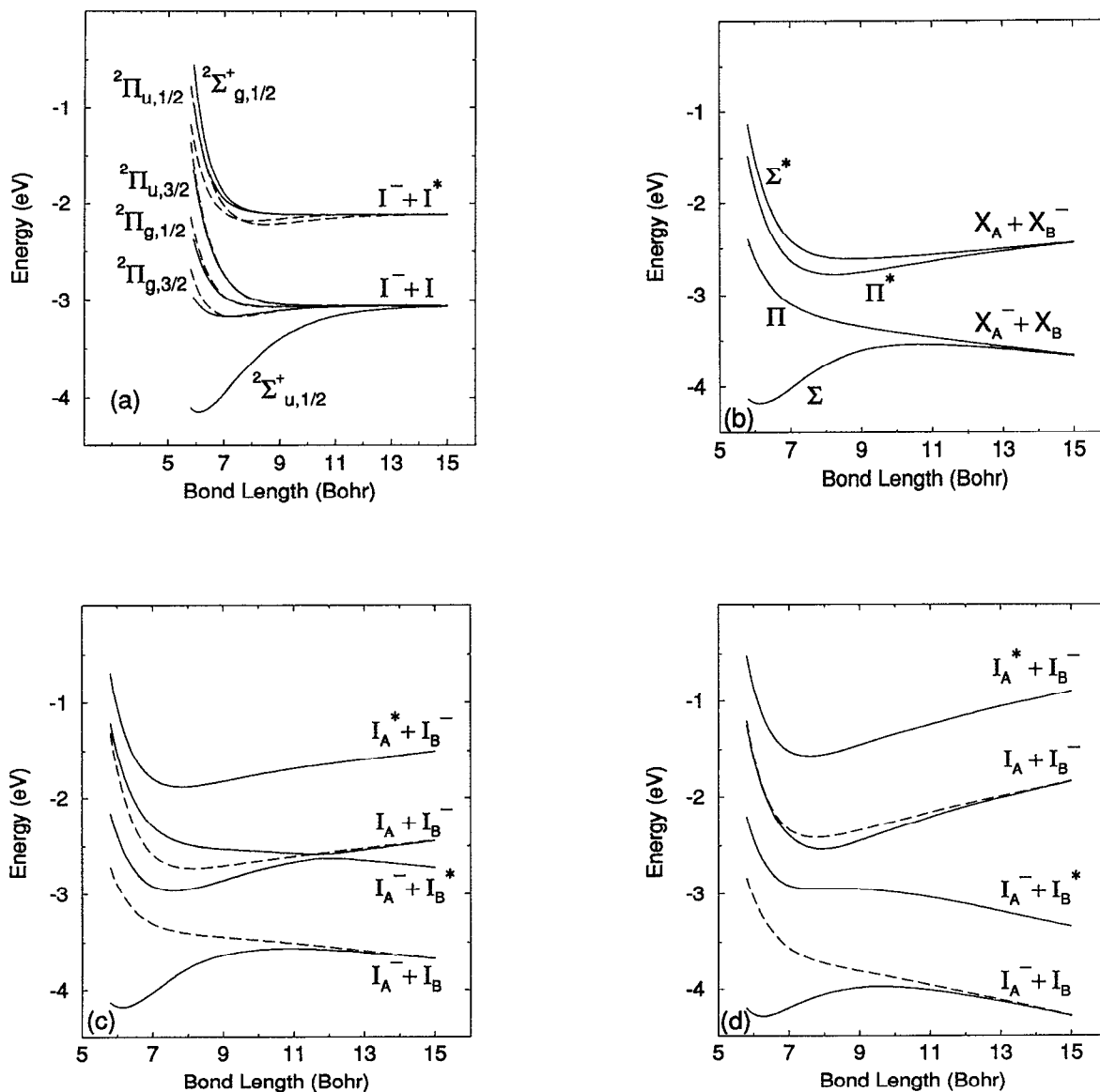


FIG. 1. Adiabatic potential energy surfaces for I_2^- . (a) Isolated I_2^- : Solid curves are the experimentally derived potentials (Ref. 18); dashed curves are the best fit of the valence bond model described in Secs. II and IV to the experimentally derived potentials. (b) Potential energy surfaces *omitting spin-orbit coupling* for I_2^- in an electric field of 0.003 a.u. parallel to the molecular axis. (c), (d) Potential energy surfaces including spin-orbit coupling for I_2^- in an electric field of 0.003 a.u. (c) and 0.006 a.u. (d). Solid curves represent $\Omega=1/2$ states and dashed curves represent $\Omega=3/2$ states. A and B denote the two iodine nuclei. The applied field points from A to B . I^* indicates iodine in the high spin-orbit energy configuration and I the low spin-orbit energy configuration. Σ and Π denote "bonding" states, Σ^* and Π^* denote "antibonding" states. Σ and Π are only good quantum numbers in the absence of spin-orbit coupling (b). Ω , the component of (spin+orbit) angular momentum along the molecular axis, is a good quantum number in all cases and is designated by the subscripts 1/2 and 3/2. The zero of energy has been chosen to coincide with dissociated I_2 (neutral) in the ground electronic state at zero field. The energy of an ion in an electric field depends on the origin of the coordinate system. For (b)–(d), the origin is at the nuclear center of mass.

ever, we anticipate that the gross distortion of the excess negative charge in I_2^- is insensitive to the details of the interaction potential, and is largely determined by the potential difference between the iodine nuclei (ΔU). In this case, a uniform field (F) of a strength which reproduces the cluster-induced potential difference between the iodine nuclei should provide a reasonable model of solvation. We have obtained a range of typical cluster-induced potential differences from earlier molecular dynamics simulations,¹⁷ and derived the corresponding field strengths from them via

$$F = \Delta U / R,$$

where R is the bond length of I_2^- . A similar approach to solvation effects is common in studies of bulk liquid solvents, where the potential energy surface for the system is a function of the solute geometry and a one-dimensional "solute coordinate."

The outline of the paper is as follows.

The model Hamiltonian which describes the $I_2^- \leftrightarrow (CO_2)_n$ interaction potential is outlined in Sec. II. It requires the matrix elements of the interaction potential in the many-electron basis of electronic eigenfunctions of isolated I_2^- . However, for the special case where the interaction potential

is a weak, uniform electric field it is remarkably easy to calculate approximate matrix elements without any knowledge of the eigenfunctions of I_2^- [Eq. (2)].

While the weak field Hamiltonian does capture the essence of the model, its extension to include arbitrary electrostatic interactions requires matrix elements of the electrostatic interaction with respect to the many-electron eigenfunctions of isolated I_2^- . These eigenfunctions have a relatively complicated form, owing to strong spin-orbit coupling in I_2^- . Furthermore, the weak field Hamiltonian breaks down for medium or strong uniform electric fields, because the assumption that certain matrix elements are negligibly small is no longer valid. For these cases, the electrostatic, spin-orbit and bonding interactions must all be treated on an equal footing. This is more involved than the weak field case, requiring explicit consideration of the wave function for I_2^- , and a full description of the interaction Hamiltonian is deferred to Sec. IV.

Uses and limitations of the model are discussed in Sec. III, and a comparison is made with *ab initio* results.

The symmetry labels for both isolated and solvated I_2^- are summarized in Sec. IV A, while the experimentally derived¹⁸ potential energy surfaces for isolated I_2^- are reviewed in Sec. IV B. The details of the model, including the basis functions, fitted parameters and fitting procedure, are contained in Secs. IV C–IV E.

The Hamiltonian for I_2^- in the presence of an arbitrary discrete charge distribution is given by Eq. (20). It requires the matrix elements of the Coulombic interaction potential with respect to a one-electron atomic orbital basis centered on the iodine nuclei. The Hamiltonian for the important special case of I_2^- subject to a uniform field, including weak, medium and strong electric fields, is given explicitly in Eq. (23). The uniform field Hamiltonian is easy to construct, with the matrix elements being linear in the electric field and linear and exponential functions of the bond length, and is valid for a much wider range of electric field strengths than the weak field Hamiltonian [Eq. (2)].

Section IV F addresses the application of the model to molecular dynamics simulations of $I_2^-(CO_2)_n$, including formulas for the forces and electronic surface hopping probabilities.

Potential energy surfaces and a charge switching function for I_2^- subject to a uniform electric field are presented in Sec. V, together with a discussion of nonadiabatic relaxation mechanisms for electronically excited I_2^- in a $I_2^-(CO_2)_n$ cluster. While no quantitative conclusions can be drawn about nonadiabatic relaxation rates in $I_2^-(CO_2)_n$ from the uniform field calculations, this preliminary study does suggest several plausible relaxation mechanisms which we hope to investigate via molecular dynamics simulations of the entire cluster.

II. MODEL HAMILTONIAN FOR I_2^- IN A WEAKLY INTERACTING SOLVENT

The simplest approach to the $I_2^- \leftrightarrow (CO_2)_n$ interaction is to treat it as a perturbation to isolated I_2^- . The zeroth order Hamiltonian matrix contains the Born–Oppenheimer potential energies of the six low-lying states of isolated I_2^- as the diagonal elements. Each CO_2 molecule is regarded as a rigid,

nonpolarizable charge distribution which is approximated by five fixed point charges. The point charges reproduce the quadrupole and hexadecapole of CO_2 .²⁶ To obtain the electronic Hamiltonian for $I_2^-(CO_2)_n$, the matrix elements of the $I_2^- \leftrightarrow (CO_2)_n$ interaction potential are added to the zeroth-order Hamiltonian matrix. The basis functions used to evaluate the matrix elements are the six electronic eigenfunctions of isolated I_2^- . (To provide an adequate description of the interaction potential at short range, intermolecular $1/R^{12}$ repulsive terms must be added to the potential. However, since these depend only on the nuclear coordinates they can be treated separately from the electronic Hamiltonian.) Either the experimentally determined¹⁸ or *ab initio* Born–Oppenheimer surfaces for isolated I_2^- can be used for the diagonal elements of the electronic Hamiltonian and any electrostatic perturbation can be treated provided the matrix elements of the perturbation are known.

For the special case of I_2^- in a uniform field F parallel to the molecular axis (z), an approximate Hamiltonian can be constructed using only the bond length R and six potential energy surfaces $E_i(R)$ for isolated I_2^- [Fig. 1(a)]. This is best illustrated by considering the two lowest eigenfunctions of I_2^- , which are formed from the degenerate basis functions $|I^-I^- \rangle$ and $|I-I^- \rangle$. Each basis function has the negative charge localized in one of the three valence $5p$ atomic orbitals, and the corresponding atomic orbital on the other iodine atom is empty. Although the basis functions are not orthogonal, the results of crude, semiempirical calculations are usually insensitive to the overlap and it is commonly neglected.²⁷ The Hamiltonian matrix for isolated I_2^- in this localized basis is

$$\begin{pmatrix} \alpha & \beta \\ \beta & \alpha \end{pmatrix}$$

where $\alpha(R)$ and $\beta(R)$ represent the diagonal and off-diagonal matrix elements of the Hamiltonian operator. The two diagonal matrix elements are equal by symmetry. In the presence of an electric field $F\hat{z}$ the basis functions $|I^-I^- \rangle$ and $|I-I^- \rangle$ are no longer degenerate and, as observed by Mulliken,²⁴ the diagonal matrix elements of \hat{z} are equal to $\pm R/2$, the position of the negative charge in the localized basis functions relative to the center of mass. The Hamiltonian matrix for I_2^- in a uniform field then becomes

$$\begin{pmatrix} \alpha - FR/2 & \beta \\ \beta & \alpha + FR/2 \end{pmatrix}$$

where the off-diagonal matrix element of $F\hat{z}$ is zero by symmetry, since \hat{z} is clearly odd in z , whereas $\langle I^-I^-(z) | I-I^-(z) \rangle$ is even. To make full use of the symmetry of the system we transform to a delocalized basis,

$$\frac{1}{\sqrt{2}} (|I^-I^- \rangle \pm |I-I^- \rangle).$$

The Hamiltonian matrix in the delocalized basis is,

$$\begin{pmatrix} \alpha + \beta & -\frac{FR}{2} \\ -\frac{FR}{2} & \alpha - \beta \end{pmatrix}, \quad \begin{pmatrix} E_u & -\frac{FR}{2} \\ -\frac{FR}{2} & E_g \end{pmatrix}.$$

At zero field the Hamiltonian matrix is diagonal, with the diagonal elements corresponding to the eigenvalues of isolated I_2^- . The eigenvalues of isolated I_2^- are customarily labeled E_u and E_g , where u/g specify the ungerade/gerade symmetry of the state. In this notation the Hamiltonian matrix is¹⁷

The above procedure is readily extended to include all six states of I_2^- , with each of the three $5p$ atomic orbitals on the two iodine nuclei contributing a g/u pair of states,

$$H(R) \sim \begin{pmatrix} E_{2\Sigma_u^+} & -\frac{FR}{2} & & & & \\ -\frac{FR}{2} & E_{2\Pi_{g,1/2}} & & & & \\ & & E_{2\Pi_{u,1/2}} & -\frac{FR}{2} & & \\ & & -\frac{FR}{2} & E_{2\Sigma_g^+} & & \\ & & & & E_{2\Pi_{g,3/2}} & -\frac{FR}{2} \\ & & & & -\frac{FR}{2} & E_{2\Pi_{u,3/2}} \end{pmatrix}. \quad (2)$$

The Σ and Π labels attached to the six potential surfaces of isolated I_2^- are not good symmetry labels. Owing to (strong) spin-orbit mixing, the only rigorous symmetry label is the quantum number $\Omega=(1/2,3/2)$, which denotes the component of (spin+electronic) angular momentum along the molecular axis. At long bond lengths and zero field the two $\Omega=1/2$ blocks correspond to the high and low spin-orbit states of iodine, with the $E_{2\Pi_{u,1/2}}$ and $E_{2\Sigma_g^+}$ states being near degenerate and separated from the near degenerate $E_{2\Sigma_u^+}$ and $E_{2\Pi_{g,1/2}}$ states by the atomic spin-orbit splitting. In this limit the eigenvalues are much more sensitive to field-dependent terms coupling the near degenerate E_i 's within each 2×2 block than to field-dependent terms between the $\Omega=1/2$ blocks, and the terms coupling different blocks can be neglected provided the field is weak. Physically, the field-dependent terms coupling the two $\Omega=1/2$ blocks can be neglected providing the singly occupied molecular orbital in each eigenfunction is well described by a linear combination of two identical Hund's case (c) atomic orbitals, one on each iodine nucleus.

The approximations used to derive the field-dependent matrix elements for Eq. (2) (the weak field Hamiltonian) are expected to break down if bonding or electric field effects are of similar magnitude to the atomic spin-orbit splitting of 0.94 eV. The breakdown of the weak field Hamiltonian when bonding effects outweigh spin-orbit coupling

is readily demonstrated. The matrix element $F\langle^2\Sigma_u^+|z|^2\Pi_{g,1/2}\rangle$, which correlates with $F\langle^2\Sigma_u^+|z|^2\Pi_g\rangle$ when spin-orbit effects are negligible, is zero by symmetry in the Hund's case (a) limit. However, in Eq. (2) this matrix element has the value $-FR/2$, regardless of the relative strength of bonding and spin-orbit coupling. Since the binding energy of the ground electronic state of I_2^- (1.1 eV) is comparable to the atomic spin-orbit splitting energy (0.94 eV), Eq. (2) is expected to provide a poor description of electric field effects for the equilibrium geometry. In addition, an applied electric field can tune into resonance atomic orbitals on opposite iodine nuclei which are not degenerate at zero field, and this effect is not described by Eq. (2). These field-induced resonances are the focus of Sec. V.

To broaden the applicability of the model Hamiltonian a more accurate expression for the R -dependent matrix elements of the electrostatic interaction is necessary. Unfortunately, this is difficult to derive because the basis functions (the eigenfunctions for isolated I_2^-) are complicated functions of R , owing to the competition between spin-orbit and bonding effects. The $^2\Pi_{g,1/2}$ state [Fig. 1(a)] provides an excellent example, with the character of the wave function ranging from almost pure Π at short bond lengths ($R \ll R_e$) to $1/3\Pi$ and $2/3\Sigma$ at longer bond lengths [Eq. (10)]. For a general electrostatic perturbation a further complication arises because each component of the six degenerate eigenfunctions is coupled to both components of the other five degenerate

functions. Although these additional matrix elements do not remove the double degeneracy of the six eigenvalues (Sec. IV A), the Hamiltonian no longer factors into two 6×6 blocks, and a 12×12 matrix must be constructed.

To minimize these problems we construct the Hamiltonian in the simpler Hund's case (a) basis. The method is briefly outlined here, and the details are given in Sec. IV. The zeroth-order Hamiltonian corresponds to isolated I_2^- , omitting spin-orbit effects (Sec. IV E). It consists of two identical, diagonal 6×6 blocks, with the basis functions in one block having α spin and those in the other block having β spin. Both spin-orbit coupling [Eq. (22)] and the electrostatic interaction [Eqs. (14) and (24)] are described by approximate matrix elements in the 12×12 electronic Hamiltonian [Eqs. (20) and (23)]. Only the spin-orbit operator has matrix elements connecting basis functions of α spin with basis functions of β spin.

The model displays the correct limiting behavior when either spin-orbit coupling or $I \cdots I$ bonding effects are dominant and it also describes field-induced resonances. The model provides a less accurate description of the wave function for I_2^- at short $I \cdots I$ bond lengths, because the atomic orbital basis includes only valence $5p$ functions and neglects polarization functions ($5s, 5d \dots$). It is not exactly equivalent to the procedure defined by Eq. (2), since the spin-orbit matrix elements are only evaluated approximately. Equation (2) above for I_2^- in a weak uniform field does capture the essence of the model, with the caveat that the field-dependent matrix elements are too approximate for many applications and cannot easily be extended to describe non-uniform fields and other solvent effects.

The model requires zeroth-order potential energy surfaces for I_2^- which omit the effects of spin-orbit coupling, so it is ideally suited to use with *ab initio* calculations (which often omit spin-orbit coupling).²⁸ A useful result, given in Sec. IV E, is that the parameters which describe the zeroth-order potential energy surfaces can be fitted one at a time to *experimental* potential energy surfaces which include the effects of spin-orbit coupling. This avoids the instability associated with multidimensional fitting.

I_2^- is just one electron short of the noble gas configuration Xe_2 , and the one hole nature of the wave function can be exploited to make approximate predictions of a variety of properties. These include solvent effects on the electronic spectrum of I_2^- and electronic surface hopping matrix elements (Sec. IV D). In particular the model enables the use of a consistent set of forces, charges and surface-hopping matrix elements (Secs. IV E and IV F) for molecular dynamics simulations of $I_2^-(CO_2)_n$. This is an improvement over earlier models^{3,13,12} which set the polarizability of I_2^- to be zero²⁹ when calculating the forces between I_2^- and the CO_2 molecules. These previous models also approximated the electronic charge distribution of I_2^- by point charges on each nucleus. In addition, they either ignored electronic surface hopping or assumed that it occurs with unit probability at a

fixed bond length. The model charge switching functions and field dependent potential energy surfaces for the excited electronic states, described in Sec. V, are quite unusual and may have ramifications for the rate of $I^* \rightarrow I$ relaxation in I_2^- .

While treatment of I_2^- in a nonuniform field requires an explicit choice of basis functions for the Hamiltonian matrix, many properties are insensitive to the precise form of the basis functions. The most important property to reproduce correctly is the quadrupole of the valence p orbital of atomic iodine, since it can interact with an external field gradient and occurs in the next term in the expansion of the $I_2^- \leftrightarrow CO_2$ interaction potential after the charge \leftrightarrow field term.

The chief virtues of our model are its simplicity and generality. As described in Sec. IV E, it actually contains fewer fitted parameters than the surfaces originally fitted to experiment,¹⁸ and it requires only trivial computations. Provided the polarizability of the solvent (CO_2) molecules is ignored, the cost of construction of the 12×12 Hamiltonian matrix scales linearly with the number of solvent molecules, while the cost of the forces and surface hopping matrix elements scales quadratically. Analytic derivatives can be used to minimize the execution time, allowing quite a large number of solvent molecules to be modeled.

III. ACCURACY AND LIMITATIONS OF THE MODEL

We now turn to a discussion of the accuracy and limitations of the model. All the results in this paper, including those for I_2^- in a uniform field, are based on the method described in Sec. IV [Eqs. (20) and (23)], rather than on Eq. (2).

The model has been fitted to small basis *ab initio* MRCI calculations,¹⁹ with spin-orbit coupling omitted from both the *ab initio* calculations and the model. It reproduces the *ab initio* parallel polarizability to within 10% and the *ab initio* (Mulliken) charges²⁰ on each atom to within 2% for electric fields in the experimental range (0–0.01 a.u.) for the $^2\Sigma_u^+$ and $^2\Pi_g$ states. The agreement seems surprisingly good, given that the parameters are fitted at zero field, though it may be an artifact of the small basis set used in the *ab initio* calculation and the omission of spin-orbit coupling from both the *ab initio* calculation and the model. However, the model also reproduces large basis (VTZ SPDF/SPD) all-electron CAS-SCF¹⁹ calculations for the $^2\Sigma_u^+$ and $^2\Pi_g$ states of Cl_2^- to a similar accuracy. The close agreement between the *ab initio* and model atomic charges on each iodine atom in the presence of a uniform electric field is a consequence of the very large parallel polarizability of I_2^- relative to I_2 . Properties of I_2^- which are chiefly determined by the drift of charge along the molecular axis are easily reproduced by a crude wave function. Both Mulliken²⁴ and Demkov^{31,32} have successfully used analytic methods to study charge switching in similar systems. The 10% error in the model polarizabilities is mainly due to the neglect of the polarizability of the iodine cores.

The model is unlikely to perform so well for properties which are sensitive to the finer details of the wave function such as electron drift perpendicular to the molecular axis or polarization of the iodine core orbitals. Electronic surface

TABLE I. Descent in symmetry for *electronic* states of iodine and I_2^- . The term symbols for atomic iodine are listed. For the group $C_{\infty v}$ and its subgroups I_2^- has two states of the same symmetry for each state of atomic iodine. For the point group $D_{\infty h}$ the states of I_2^- occur in gerade/ungerade pairs.

Group	Orbital symmetry	\otimes	Spin symmetry	\mapsto	Total symmetry	Symmetry operators ^a
K	$P(\equiv D_1)$		$D_{1/2}$		$D_{1/2} \oplus D_{3/2}$	J_a, J_z , time reversal
$C_{\infty v}$	$\Sigma^+ \oplus \Pi$		$E_{1/2}$		$E_{1/2} \oplus (E_{1/2} \oplus E_{3/2})$	J_z , time reversal
C_s	$A' \oplus (A' \oplus A'')$		$E_{1/2}$		$3E_{1/2}$	time reversal
C_1	$3A$		$2B_{1/2}$		$6B_{1/2}$	time reversal

^aSymmetry operators of the total Hamiltonian, including the spin-orbit Hamiltonian. J_z is the projection of the (spin+electronic) angular momentum along the molecular axis, with eigenvalues Ω . For the isolated atom the total (spin+electronic) angular momentum J_a is also conserved.

hopping between $\Omega=1/2$ and $\Omega=3/2$ states depends on both of these properties, so it will not be predicted accurately. Coupling of the low lying electronic states of isolated I_2^- to the highly excited states by the $I_2^- \leftrightarrow CO_2$ interaction, which accounts for the polarization of the iodine cores, occurs at the next order of perturbation theory and is not treated here. Truncation at the lower order is justified provided the perturbation does not strongly couple the six nearly degenerate states to the highly excited states.³³ Since the first electronically excited state of I_2^- is very close to the ionization limit, strong solvent coupling of the low-lying states to the other states would be expected to cause significant delocalization of the outermost electron into the solvent. Experiments on I^- in CO_2 clusters indicate that only a small amount of delocalization occurs,³⁴ so omission of these effects is probably a reasonable approximation.

Throughout this paper, the polarizability of the CO_2 solvent is ignored, even though it does affect the electronic structure of I_2^- . This has been done in the interests of simplicity. While the polarizability of the solvent has been included in molecular dynamics simulations of $Br_2^-(CO_2)_n$,¹² it is considerably harder to include the solvent-solute polarizability interactions in a consistent manner. Several authors, notably Kim and Hynes³⁵ and Gertner and Hynes,¹⁶ have successfully treated solvent-solute polarizability interactions in related systems and we are currently working on this. If one treats the solvent-solute interaction using Van Vleck degenerate perturbation theory,³³ with the zeroth-order Hamiltonian corresponding to the isolated solute, the model presented here considers all terms to first order, while solvent polarization effects enter at second order. (The latter point is related to the definition of polarizability as the *second* derivative of the Born-Oppenheimer energy with respect to electric field.)

Since each CO_2 molecule is approximated by a finite number of point charges or multipoles, the model Hamiltonian also neglects chemical bonding interactions between I_2^- and CO_2 . This is a major limitation of the model and yet it is precisely this approximation which makes it feasible to extend the calculations to larger clusters of experimental interest. For the case of $I_2^-(CO_2)_n$, bonding between I_2^- and the CO_2 molecules is expected to be very weak because CO_2 has a *negative* electron affinity while I^- has an ionization potential of 3.14 eV. Also, assuming CO_2 is more likely to bond to I^- than to neutral I, the impact of bonding on electronic

relaxation may be small because I^- is closed shell and can only cause electronic transitions indirectly by its influence on open shell iodine. Nevertheless, at first sight it seems a gross approximation to neglect bonding interactions during a collision of a CO_2 molecule with I_2^- . However, the enormous difference in the ionization potentials of I_2^- (3.06 eV)¹⁸ and CO_2 (13.769 eV),³⁶ together with the negative electron affinity of CO_2 , suggest that the valence orbitals of I_2^- are *too diffuse* to undergo chemical bonding with the valence orbitals of CO_2 , even at close range. The short range repulsive potential between I_2^- and CO_2 , which we presume to be due to interactions of the CO_2 valence orbitals with I_2^- core orbitals of similar energy, is described empirically by adding a $1/R^{12}$ repulsive term to the Hamiltonian. For cases where bonding forces between I_2^- and a solvent are significant it may prove feasible to construct a wave function for the entire cluster from the wave functions for each diatomic fragment using the semiempirical diatomics-in-molecules approach.^{37,38}

IV. DETAILS OF THE MODEL HAMILTONIAN

A. Symmetry labels for I_2^-

The six model potential energy surfaces for I_2^- described in the Sec. IV E are applicable to I_2^- in a uniform or nonuniform electric field or in a solvent, and the electronic symmetry labels for each situation are summarized below.

The symmetry labels for the ground $5s^25p^5$ configuration of *atomic* iodine, which is one electron short of the noble gas configuration of xenon, can be deduced by treating it as a one hole system, so the term symbols are the same as for the hydrogen atom. The term symbols for I_2^- classified in the $C_{\infty v}$ point group can be obtained easily³⁹ by forming the direct product of the term symbols for I with those of I^- . Since the ground electronic state of I^- is totally symmetric in the $C_{\infty v}$ group, the term symbols for I_2^- are identical to those of atomic iodine classified according to $C_{\infty v}$. In the $5s^25p^5$ configuration of iodine the hole can occupy any one of the three p orbitals and can have α or β spin, giving a total of six states. For each state of atomic iodine one can form two states of I_2^- with the same term symbol from the linear combinations ($I^- - I \pm I - I^-$). When classified according to the $D_{\infty h}$ group these 12 states also possess inversion symmetry; six states are gerade and six are ungerade.^{39,40} The symmetry labels for the spatial and spin functions for I_2^- and atomic

iodine are summarized in Table I. Owing to the strength of spin-orbit mixing it is appropriate to use the symmetry of the total *space*×*spin* wave function rather than the symmetry of the spatial function alone and this has also been included. The subscripts 1/2 and 3/2 in the term symbols for the total wave functions indicate the component of (electronic+spin) angular momentum along the molecular axis. Spin-orbit coupling can only mix functions of the same total symmetry. In iodine the $|^2\Sigma^+\alpha\rangle$ and $|^2\Pi(\Lambda=+1)\beta\rangle$ configurations are strongly mixed and the spin-orbit splitting in atomic iodine is ~ 1 eV. The 12 states of I_2^- in a vacuum are customarily labeled

$$^2\Sigma_{u,1/2}^+, \quad ^2\Pi_{g,3/2}, \quad ^2\Pi_{g,1/2}, \quad ^2\Pi_{u,3/2}, \quad ^2\Pi_{u,1/2}, \quad ^2\Sigma_{g,1/2}^+,$$

where it is understood that each state is doubly degenerate and that Σ/Π are merely convenient labels, not good quantum numbers.

Nonadiabatic electronic transitions in I_2^- are induced by movement of the nuclei or by movement of neighboring nuclei and this is reflected in a lowering of the symmetry group. Rotation of I_2^- removes the cylindrical symmetry, so the component of (electronic+orbital) angular momentum along the molecular axis, Ω , is no longer conserved. Electronic-rotation Coriolis coupling (Λ doubling) is usually weak and the rovibrational states occur in nearly degenerate pairs of opposite parity, with the two states having the same direction of nuclear rotation but opposite directions of electronic rotation about the molecular axis (Π_{\pm}).

In the point group C_1 the ground electronic configuration spans $12B_{1/2}$, so it appears that the electronic states are no longer degenerate. However, even in this case the $B_{1/2}$ states occur in degenerate pairs, because the electronic (and total) Schrödinger equation is invariant under time reversal. Kramer's theorem^{41,42} states that, because the Schrödinger equation for a system unperturbed by external magnetic fields is invariant under time reversal, every energy level of such a system with an odd number of electrons is at least doubly degenerate. Internal magnetic fields produced by molecular rotation, etc., do not split this degeneracy.⁴³ The degeneracy is most easily seen for a simple system such as the hydrogen atom. For each state, say $|1S\alpha\rangle$, there is a degenerate state of opposite spin ($|1S\beta\rangle$). Spin-orbit coupling mixes basis functions of α and β spin, so that the degeneracy is not so obvious; here, Kramer's theorem tells us that for each state we can obtain a linearly independent, degenerate state by reversing the momenta of all particles (including both space and spin coordinates). This enduring degeneracy reduces the number of electronic eigenvalues which must be considered from 12 to 6.

Parity is always a good quantum number for an isolated system, regardless of the point group symmetry of the system, though states of \pm parity do not usually occur in pairs for nonlinear systems. However, because parity, the inversion of nuclear and electronic spatial coordinates through the origin of the space fixed axis system, relates the value of the electronic wave function at one nuclear configuration to that at another nuclear configuration, it is of little use when solving the electronic Schrödinger equation for clamped nuclei.

B. Empirical potential energy surfaces for isolated I_2^-

The six s^2p^5 potential energy curves of isolated I_2^- as determined from experimental data by Chen and Wentworth¹⁸ are reproduced in Fig. 1(a). At long bond lengths the four low energy spin-orbit states (I) are displaced from the two high energy spin-orbit states (I^*) by the atomic spin-orbit splitting, while at shorter bond lengths $\Omega=1/2$ configurations from the I and I^* states are mixed by bonding between the iodine nuclei. The competing effects of bonding and spin-orbit coupling cause the excited electronic states to respond in an unusual fashion to electric fields, as discussed in Sec. V. Although the states are usually identified by Hund's case (a) labels, our model calculations suggest that spin-orbit coupling causes nearly complete mixing of $\Omega=1/2$ Σ and Π states except in the highly repulsive region below 6 Bohr. In contrast, the $\Omega=3/2$ Π states are not mixed with Σ states by spin-orbit coupling, so the Π label is applicable.

Chen and Wentworth¹⁸ fitted the available experimental data for I_2^- to six Morse potentials. While the fits for the two high spin-orbit energy I^* states were not uniquely determined by the available data, the lower four states were each fitted to three or four independent pieces of data. The undetermined parameters for the upper states were set by comparison with the values for the dihalide ions F_2^- , Cl_2^- , and Br_2^- .

C. Basis functions for the model Hamiltonian

The basis used to describe the model wave function is very simple, consisting of the three $5p$ atomic orbitals on each iodine atom. A full-configuration interaction calculation for the six degenerate states of $I_2^-(CO_2)_n$ is performed in this basis, with $I\cdots I$ bonding matrix elements approximated by semiempirical parameters. I_2^- has 11 electrons in the $5p$ valence shell, while the basis consists of only 12 spin-orbitals, so the full-C.I. wave functions are linear combinations of just 12 Hartree-Fock type determinants, each with a hole in a different spin-orbital. In order to fully specify the phase conventions adopted in the model, the following subsections contain explicit phases for the basis functions and definitions of the necessary coordinate transformations.

1. Atomic orbitals

The phases for the atomic orbitals are chosen such that the positive lobes of the real Cartesian p orbitals are directed along the positive Cartesian axes. The p orbitals can be aligned parallel to the space-fixed (XYZ) or molecule-fixed (xyz) axes.

While the electronic wave functions for isolated I_2^- are most naturally defined in a molecule-fixed axis system, molecular dynamics calculations are usually referred to space-fixed axes. To make a consistent choice of the positive direction for the molecular axis throughout a molecular dynamics simulation, we label the iodine nuclei I_A and I_B , with coordinates \mathbf{R}_A and \mathbf{R}_B . The molecular axis is defined to be $(\mathbf{R}_B - \mathbf{R}_A)$.

The molecule-fixed axes can be obtained by rotating the space-fixed axes through the Euler angles $(\phi, \theta, 0)$, $[0 \leq \phi \leq 2\pi, 0 \leq \theta \leq \pi]$. We have followed the Euler angle con-

vention defined by Zare.⁴⁴ Cartesian p orbitals aligned along the molecule-fixed axes, p_x, p_y, p_z , are related to Cartesian p orbitals aligned along the space-fixed axes, p_X, p_Y, p_Z , by the well-known direction cosine matrix $\Phi(\theta, \phi)$,

$$\begin{pmatrix} p_x \\ p_y \\ p_z \end{pmatrix} = \Phi^t(\theta, \phi) \begin{pmatrix} p_X \\ p_Y \\ p_Z \end{pmatrix}. \quad (3)$$

For many purposes it is more convenient to use a space-fixed spherical basis, p_+, p_0, p_- ,

$$\begin{pmatrix} p_x \\ p_y \\ p_z \end{pmatrix} = \mathbf{T}^t \begin{pmatrix} p_+ \\ p_0 \\ p_- \end{pmatrix}, \quad (4)$$

$$\mathbf{T} = \begin{pmatrix} -\frac{1}{\sqrt{2}} & \frac{i}{\sqrt{2}} & 0 \\ 0 & 0 & 1 \\ \frac{1}{\sqrt{2}} & \frac{i}{\sqrt{2}} & 0 \end{pmatrix}.$$

Molecule fixed (xyz) spherical basis functions are related to space fixed (XYZ) spherical basis functions by the rotation matrices of angular momentum theory⁴⁵

$$\begin{pmatrix} p_+ \\ p_0 \\ p_- \end{pmatrix}^{xyz} = \Theta^{1t}(\theta, \phi) \begin{pmatrix} p_+ \\ p_0 \\ p_- \end{pmatrix}^{XYZ}, \quad (5)$$

where

$$\Theta_{M,M'}^1(\theta, \phi) = \exp(+iM\phi) d_{M,M'}^1(\theta), \quad (6a)$$

$$\mathbf{d}^1(\theta) = \frac{1}{2} \begin{pmatrix} (1 + \cos \theta) & -\sqrt{2} \sin \theta & (1 - \cos \theta) \\ \sqrt{2} \sin \theta & \cos \theta & -\sqrt{2} \sin \theta \\ (1 - \cos \theta) & \sqrt{2} \sin \theta & (1 + \cos \theta) \end{pmatrix}. \quad (6b)$$

The Cartesian and spherical transformations are related by \mathbf{T} ,

$$\Phi = \mathbf{T}^t \Theta^t \mathbf{T}. \quad (7)$$

Twelve atomic spin-orbitals are produced from the six atomic orbitals and the two spin functions (α, β), and they form the one-electron basis for the electronic wave function of $I_2^-(\text{CO}_2)_n$. The relations between molecule-fixed and space-fixed basis functions, and between Cartesian and spherical basis functions, are summarized by the matrix equations,

$$\begin{aligned} &\text{AO(molecule fixed Cartesian spatial orbitals,} \\ &\text{space fixed spin)} \\ &= \Phi^t \text{AO(space fixed Cartesian spatial orbitals,} \\ &\text{space fixed spin)} \\ &= \mathbf{T}^t \Theta^{1t} \text{AO(space fixed spherical spatial orbitals,} \\ &\text{space fixed spin),} \end{aligned} \quad (8)$$

where \mathbf{T} , Θ^t , and Φ are now 12×12 matrices with components given by Eqs. (4), (6), and (7).

An explicit form for the p_z atomic orbital was obtained from an SCF calculation¹⁹ on atomic iodine omitting spin-orbit coupling, using a palladium effective core potential and a small sp basis of Cartesian Gaussians.^{19,22} The p_x and p_y orbitals differ from the p_z orbital only by a rotation. No allowance has been made for the distortion of the atomic orbitals which occurs as the iodine nuclei approach each other, and the p orbitals of I^- are assumed to be identical to those of neutral iodine. Polarization functions for the atomic orbitals (s, d, \dots) have been omitted for simplicity; the main objective of the model is to reproduce the gross charge drift along the z axis.

p_+, p_0 , and p_- , aligned relative to the space fixed axes, are eigenfunctions of \hat{l}_z ,

$$\hat{l}_z p_{\pm} = \pm p_{\pm}, \quad \hat{l}_z p_0 = 0. \quad (9a)$$

They also satisfy the Condon and Shortley phase convention,⁴⁶

$$\hat{l}^- p_+ = \sqrt{2} p_0, \quad \hat{l}^- p_0 = \sqrt{2} p_-, \quad (9b)$$

where $\hat{l}^- = \hat{l}_x - i\hat{l}_y$. The same equations hold for molecule fixed p_+, p_0 , and p_- , with \hat{l}_x, \hat{l}_y , and \hat{l}_z replaced by \hat{l}_x, \hat{l}_y , and \hat{l}_z . The spin functions also satisfy the Condon and Shortley phase convention,

$$\hat{s}^- \alpha = \beta \quad (9c)$$

where $\hat{s}^- = \hat{s}_x - i\hat{s}_y$.

It would be possible to use the molecule-fixed Hund's case (c) atomic orbitals $|j\Omega\rangle$ appropriate for strong spin-orbit coupling,

$$\begin{aligned} |3/2, 3/2\rangle &= p_+, \\ |3/2, 1/2\rangle &= \sqrt{2/3} p_0 + \sqrt{1/3} \bar{p}_+, \\ |1/2, 1/2\rangle &= \sqrt{1/3} p_0 - \sqrt{2/3} \bar{p}_+, \end{aligned} \quad (10)$$

where both the spin and spatial functions are aligned relative to the molecule fixed axes. These functions satisfy the Condon and Shortley phase convention for the total (spin + orbital) angular momentum,⁴⁷

$$\hat{j}^- |3/2, 3/2\rangle = \sqrt{3} |3/2, 1/2\rangle, \quad \langle 3/2, 1/2 | \hat{s}_z | 1/2, 1/2 \rangle > 0,$$

where $\hat{j}^- = \hat{s}^- + \hat{l}^-$. They are eigenfunctions of \hat{j}_z . However, the solvent-solute Hamiltonian is more easily constructed with respect to the simpler Hund's case (a) atomic orbitals. For this reason, we have endeavored to convert the Chen-Wentworth¹⁸ parametrization of the true [Hund's case (c)] potential energy surfaces for I_2^- to a Hund's case (a) parametrization, as discussed in Sec. IV E. While the Hund's case (c) atomic orbitals are not required for the construction of the Hamiltonian matrix, they are needed for calculating some properties of the electronic eigenfunctions such as the expectation value of \hat{j}_x .

2. Molecular orbitals for isolated I_2^-

If spin-orbit coupling is neglected, the molecular orbital coefficients of the 12 Cartesian, molecule-fixed atomic spin-orbitals are determined by symmetry,

$$MO_{i,u/g} = (AO_{A,i} \pm AO_{B,i}) / \sqrt{2(1 \pm \langle AO_{A,i} | AO_{B,i} \rangle)}, \quad (11a)$$

where i denotes a particular Cartesian component (x , y , or z) and a particular spin (α or β). The 12×12 matrix of molecular orbital coefficients \mathbf{C} is defined as,

$$\mathbf{MO} = \mathbf{C}^t \mathbf{AO} (\text{molecule fixed Cartesian spatial orbitals, space fixed spin}). \quad (11b)$$

3. Eleven electron determinants

Each 11-electron determinant is constructed from 11 of the 12 molecular spin-orbitals. The relative phases of the determinants are defined by specifying the column ordering

$$\{(xu), (\overline{xu}), (xg), (\overline{xg}), (yu), (\overline{yu}), (yg), (\overline{yg}), (zu), (\overline{zu}), (zg), (\overline{zg})\}, \quad (12)$$

where (\overline{xu}) is short hand for $\overline{MO}_{x,u}$, the ungerade molecular orbital with β spin constructed from $\overline{p}_{A,x}$ and $\overline{p}_{B,x}$.

Each determinant is labeled by the unpaired electron and the spatial symmetry (Σ^+ or Π). Thus

$$\overline{\Pi}_{y,u} = \mathcal{A}\{(xu)(\overline{xu})(xg)(\overline{xg})(yu)(\overline{yu})(yg)(\overline{yg})(zu)(\overline{zu}) \times (zg)(\overline{zg})\}.$$

D. Approximate Hamiltonian matrix elements for one electron operators

Matrix elements of several one electron operators are required by the model. In the current approximation, the $I_2^- \leftrightarrow \text{CO}_2$ interaction and the spin-orbit interaction are one electron operators. Calculation of nonadiabatic effects requires the matrix elements of the one electron operator $-i\nabla_{\mathbf{X}}$, where \mathbf{X} refers to all the nuclear degrees of freedom in $I_2^-(\text{CO}_2)_n$. It is useful to know the projection of the (spin + electronic) angular momentum of the cluster along the I-I molecular axis, \hat{j}_z , which is also a one electron operator. Explicit matrix elements for these operators are given below. Intramolecular bonding in I_2^- is also modeled by a one-electron operator, as described in Sec. IV E.

Making use of the usual rules for matrix elements of a Hermitian one electron operator \hat{A} between determinants $|i\rangle$ one obtains,

$$\langle i | \hat{A} | j \rangle = \langle \text{hole}_j | \hat{A} | \text{hole}_i \rangle \quad (i \neq j), \quad (13a)$$

$$\langle i | \hat{A} | i \rangle + \langle \text{hole}_i | \hat{A} | \text{hole}_i \rangle = \langle I_2^{2-} | \hat{A} | I_2^{2-} \rangle. \quad (13b)$$

Thus,

$$\langle i | \hat{A} | i \rangle = \langle I_2^{2-} | \hat{A} | I_2^{2-} \rangle - \langle \text{hole}_i | \hat{A} | \text{hole}_i \rangle, \quad (13c)$$

where the determinant $|i\rangle$ has a hole in the molecular spin-orbital $|\text{hole}_i\rangle$.

The rules for evaluating matrix elements of determinants require that the determinants first be rearranged such that molecular spin-orbitals common to both determinants occur

in the same column in both determinants. This can alter the sign of the off-diagonal matrix elements of \hat{A} . If the molecular spin-orbitals are ordered according to Eq. (12), the off-diagonal matrix elements have the sign,

$$\langle i | \hat{A} | j \rangle = - \langle \text{hole}_j | \hat{A} | \text{hole}_i \rangle \quad (\text{if hole}_i \text{ and hole}_j \text{ have the same spin}), \quad (13d)$$

$$\langle i | \hat{A} | j \rangle = + \langle \text{hole}_j | \hat{A} | \text{hole}_i \rangle \quad (\text{if hole}_i \text{ and hole}_j \text{ have opposite spin}). \quad (13e)$$

We now turn to the derivation of explicit expressions for the matrix elements of the one electron operators required by the model. In cases where the one electron matrix elements are derived in the atomic orbital basis, Eqs. (8) and (11) can be used to transform them to the molecular orbital basis required by Eq. (13). Approximate expressions for the many electron integral $\langle I_2^{2-} | \hat{A} | I_2^{2-} \rangle$ are obtained by exploiting the fact that I_2^{2-} has a closed-shell wave function.

1. Spin-orbit interaction

The spin-orbit Hamiltonian is approximated by a one electron operator,⁴⁸

$$H^{\text{so}} = \hat{a} \{ \hat{l}_z \hat{s}_z + \frac{1}{2} (\hat{l}^+ \hat{s}^- + \hat{l}^- \hat{s}^+) \}.$$

In a further approximation, integrals between atomic orbitals on different nuclei are assumed to be zero because \hat{a} , which is only a function of the spatial coordinates, decays rapidly ($1/r^3$) as the electron moves away from the nucleus. Only the one center, one electron atomic orbital integrals are calculated, and the spin-orbit operator for each one center integral is taken to be that for the isolated atom.

Spin-orbit effects cancel for doubly occupied orbitals, so the matrix element involving I_2^{2-} is zero. The integrals over *space fixed spherical atomic spin-orbitals* can be reduced to integrals over spatial functions alone by making use of the properties of angular momentum eigenfunctions [Eq. (9)],

$$\langle p_+ | H^{\text{so}} | p_+ \rangle = + \frac{1}{2} \langle p_+ | \hat{a} | p_+ \rangle,$$

$$\langle \bar{p}_- | H^{\text{so}} | \bar{p}_- \rangle = + \frac{1}{2} \langle \bar{p}_- | \hat{a} | \bar{p}_- \rangle,$$

$$\langle \bar{p}_+ | H^{\text{so}} | \bar{p}_+ \rangle = - \frac{1}{2} \langle \bar{p}_+ | \hat{a} | \bar{p}_+ \rangle,$$

$$\langle p_- | H^{\text{so}} | p_- \rangle = - \frac{1}{2} \langle p_- | \hat{a} | p_- \rangle,$$

$$\langle \bar{p}_0 | H^{\text{so}} | p_- \rangle = + \frac{1}{\sqrt{2}} \langle p_0 | \hat{a} | p_0 \rangle,$$

$$\langle p_0 | H^{\text{so}} | \bar{p}_+ \rangle = + \frac{1}{\sqrt{2}} \langle p_0 | \hat{a} | p_0 \rangle, \quad \langle p_0 | H^{\text{so}} | p_0 \rangle = 0.$$

The matrix elements over spatial functions are set equal to the spin-orbit coupling constant for atomic iodine.⁴⁸ The operator \hat{a} is positive everywhere,⁴⁸ so we set

$$\langle p_+ | \hat{a} | p_+ \rangle = \langle p_0 | \hat{a} | p_0 \rangle = \langle p_- | \hat{a} | p_- \rangle = + 5068 \text{ cm}^{-1}.$$

2. I_2^- in a uniform electric field

If the field F is parallel to the molecular (z) axis and the origin is taken to be the center of mass ($z_{c.m.}$),

$$\hat{F} = F(\hat{z} - z_{c.m.}),$$

$$\langle I_2^{2-} | \hat{F} | I_2^{2-} \rangle = 0 \quad (\text{by symmetry}).$$

The nonvanishing one electron integrals, expressed in the *molecule fixed Cartesian atomic orbital basis*, are

$$\langle p_{A,i} | \hat{F} | p_{A,i} \rangle = -\frac{1}{2}FR \quad (i = x, y, z),$$

$$\langle p_{B,i} | \hat{F} | p_{B,i} \rangle = +\frac{1}{2}FR \quad (i = x, y, z),$$

where R is the I–I bond length, and similarly for atomic spin-orbitals with spin β .

3. General $I_2^- \leftrightarrow (CO_2)_n$ interaction

For the general case of I_2^- surrounded by an arbitrary number (n) of CO_2 molecules represented by charges Q_k at positions \mathbf{X}_k , the $I_2^- \leftrightarrow (CO_2)_n$ interaction Hamiltonian is

$$\sum_{k=1}^n \frac{Q_k}{|\mathbf{r} - \mathbf{X}_k|} \quad (14)$$

where \mathbf{r} is the electronic coordinate. The operator is readily generalized to include point multipoles of arbitrary order. Each Hamiltonian matrix element $\langle i | \sum_{k=1}^n (Q_k / |\mathbf{r} - \mathbf{X}_k|) | j \rangle$ can be written as a sum of n terms of the form $Q_k \langle i | 1/|\mathbf{r} - \mathbf{X}_k| | j \rangle$. Using Eq. (13) these integrals are expressed in terms of the one electron integrals $\langle \text{hole}_j | 1/|\mathbf{r} - \mathbf{X}_k| | \text{hole}_i \rangle$ and the many electron integral $\langle I_2^{2-} | 1/|\mathbf{r} - \mathbf{X}_k| | I_2^{2-} \rangle$. The former is just the familiar nuclear attraction integral³⁰ commonly encountered in *ab initio* calculations. It is evaluated exactly via standard methods in the *space fixed Cartesian (Gaussian) atomic orbital basis*, using an explicit form for the atomic orbitals. The integral $\langle I_2^{2-} | 1/|\mathbf{r} - \mathbf{X}_k| | I_2^{2-} \rangle$ is the electrostatic potential of I_2^{2-} at position \mathbf{X}_k . If \mathbf{X}_k is outside the I_2^{2-} charge cloud, it is simply the coulomb repulsion energy between a unit charge (a.u.) at position \mathbf{X}_k , and charges of -1 coincident with the iodine nuclei. (This assumes that the wave function for I_2^{2-} is simply the product of the wave functions for isolated I_A^- and I_B^- , which is consistent with the neglect of orbital polarization for I_2^-). If charge Q_k penetrates the I_2^{2-} charge cloud of atom I_A , then the charge on I_A is reduced to the charge enclosed in a sphere centered at A touching \mathbf{X}_k . Thus matrix elements of arbitrary electrostatic potentials require the radial potential function for isolated (spherical) I^- ; this has been calculated at the SCF level.¹⁹ In practice the CO_2 molecules can only penetrate a small distance into the I_2^- charge cloud before encountering a short range repulsive (Lennard-Jones) potential, described in the Appendix, and neglect of penetration effects has only a marginal effect on the $I_2^- \leftrightarrow (CO_2)_n$ interaction potential.

4. Nonadiabatic interaction

The semi-classical description of electronic surface hopping requires the matrix elements of the gradient operator (Sec. IV F),

$$\hat{P} = -i\nabla_{\mathbf{X}},$$

where \mathbf{X} spans all $3N$ nuclear coordinates. \hat{P} represents the momentum of the nuclei and hence is Hermitian. It follows that $\nabla_{\mathbf{X}}$ is skew-Hermitian. In the following we consider a single component, $\hat{P} = d/dX$.

For any normalized function ψ it is easy to show that $\langle \psi | d/dX \psi \rangle$ is a pure imaginary number by differentiating the normalization condition, $\langle \psi | \psi \rangle = 1$. If ψ is real then the expectation value of d/dX is zero. For complex ψ the pure imaginary term $\langle \psi | d/dX \psi \rangle$ determines how the phase of ψ varies as nuclear coordinate X is displaced, and we are free to choose the phase such that

$$\langle \psi | d/dX \psi \rangle = 0 \quad \text{for all } \psi.$$

In particular,

$$\langle I_2^{2-} | d/dX | I_2^{2-} \rangle = 0.$$

The one electron matrix elements are most easily evaluated in the *space fixed Cartesian atomic orbital basis*, with the transformation to molecular orbitals defined by Eqs. (7), (8), and (11),

$$\mathbf{MO} = \mathbf{C}^t \mathbf{T}^t \mathbf{\Theta}^t \mathbf{T}^* \mathbf{AO}$$

(space fixed Cartesian spatial orbitals,
space fixed spin).

Evaluation of $d\mathbf{MO}/dX$ requires $d\mathbf{C}/dX$, $d\mathbf{T}/dX$, $d\mathbf{\Theta}^t/dX$ and $d\mathbf{AO}/dX$. \mathbf{T} is a constant matrix [Eq. (4)], so $d\mathbf{T}/dX = 0$. The derivatives of the atomic orbitals, $d\mathbf{AO}/dX$, give rise to small but spurious nonadiabatic transitions for an isolated particle moving at constant velocity, and it is common practice to set them equal to zero, as discussed in Sec. IV F. \mathbf{C} depends only upon the I–I bond length R [Eq. (11)], so

$$\frac{d\mathbf{C}}{dX} = \frac{d\mathbf{C}}{dR} \frac{dR}{dX},$$

$d\mathbf{C}/dR$ reduces to the derivative of the overlap of (molecule fixed) atomic orbitals centered on I_A and I_B . The atomic orbital overlap is approximately exponential in R , and a single exponential has been fitted to the *ab initio* overlap, as described in Sec. IV E. Similarly,

$$\frac{d\mathbf{\Theta}^t(\theta, \phi)}{dX} = \frac{d\mathbf{\Theta}^t}{d\theta} \frac{d\theta}{dX} + \frac{d\mathbf{\Theta}^t}{d\phi} \frac{d\phi}{dX}.$$

The derivatives of $\mathbf{\Theta}^t$ are obtained from Eq. (6). $d\theta/dX$, $d\phi/dX$, and dR/dX are obtained by differentiating Eq. (3) for the special case,

$$\begin{pmatrix} p_x \\ p_y \\ p_z \end{pmatrix} = \begin{pmatrix} 0 \\ 0 \\ R \end{pmatrix}, \quad \begin{pmatrix} p_X \\ p_Y \\ p_Z \end{pmatrix} = \begin{pmatrix} X_B - X_A \\ Y_B - Y_A \\ Z_B - Z_A \end{pmatrix},$$

where X_A and X_B are the X coordinates of nuclei I_A and I_B and $\Phi(\theta, \phi)$ is given explicitly in Eq. (7). The derivatives $d\Theta^1/dX$, which are only nonzero if the nuclear coordinate X belongs to one of the iodine nuclei, describe Coriolis (electron-nuclear rotation) coupling in I_2^- .

5. Angular momentum matrix elements

The component of (spin+electronic) angular momentum along the molecular axis, \hat{j}_z , is a good quantum number for isolated I_2^- , with allowed values $\pm 1/2, \pm 3/2$ for the lowest six electronic states. The expectation value of \hat{j}_z for the electronic wave function of $I_2^-(CO_2)_n$ provides a useful measure of the strength of the cluster-induced $1/2 \leftrightarrow 3/2$ mixing.

The matrix elements of \hat{j}_z are readily evaluated in the *molecule fixed Hund's case (c) atomic orbital basis* [Eq. (10)], reducing to simple atomic orbital overlaps, since these orbitals are eigenfunctions of \hat{j}_z .

Transformation from the atomic orbital basis to the molecular orbital basis requires a transformation of both the spatial functions and the spin functions. The transformation of the (molecule fixed) spatial functions from a spherical basis to a Cartesian basis is readily performed with reference to Eqs. (4), (8), and (11),

$$\mathbf{MO} = \mathbf{C}^t \mathbf{T}^t \mathbf{AO}$$

(molecule fixed spherical spatial orbitals,
space fixed spin).

Transformation from the space-fixed (XYZ) spin basis to the molecule-fixed (xyz) spin basis⁴⁵ closely resembles the transformation of spherical p orbitals [Eqs. (5) and (6)],

$$\begin{pmatrix} \alpha \\ \beta \end{pmatrix}^{xyz} = \Theta^{1/2}(\theta, \phi) \begin{pmatrix} \alpha \\ \beta \end{pmatrix}^{XYZ}, \quad (15a)$$

where

$$\Theta_{M, M'}^{1/2}(\theta, \phi) = \exp(+iM\phi) d_{M, M'}^{1/2}(\theta), \quad (15b)$$

$$\mathbf{d}^{1/2}(\theta) = \begin{pmatrix} \cos(\theta/2) & -\sin(\theta/2) \\ \sin(\theta/2) & \cos(\theta/2) \end{pmatrix}. \quad (15c)$$

Thus,

$$\mathbf{MO} = \mathbf{C}^t \mathbf{T}^t \Theta^{1/2*} \mathbf{AO}$$

(molecule fixed spherical spatial orbitals,
molecule fixed spin),

where $\Theta^{1/2}$ is now a 12×12 matrix with components given by Eq. (15). Finally, the transformation of these atomic orbitals to the (molecule fixed) Hund's case (c) atomic orbitals is given by Eq. (10).

Because α and β have half-integral spin, the domain of θ and ϕ is doubled, to 2π and 4π respectively. If the domain of

the Euler angles is restricted to that appropriate for integral angular momentum then, owing to the fact that a rotation of 2π changes the sign of α and β ,

$$\Theta^{1/2}(2\pi + \theta, \phi) = \Theta^{1/2}(\theta, 2\pi + \phi) = -\Theta^{1/2}(\theta, \phi)$$

and all the molecular orbitals may be in error by the same phase factor of -1 . However, the erroneous phase factor is the same for all the molecular orbitals, so it has no effect on matrix elements.

E. Fitted parameters for the I_2^- potential

1. Definition of the bonding parameters

If the intramolecular $I \cdots I$ bonding interaction in I_2^- is assumed to be a one electron operator, H^{bonding} , then the fitting equations for the bonding parameters take a very simple form. The ansatz that H^{bonding} is a one electron operator can be motivated by comparison with the Fock operator which defines the Hartree-Fock wave function and is a pseudo one electron operator. The bonding Hamiltonian H^{bonding} is defined to be the total electronic Hamiltonian for I_2^- , omitting spin-orbit coupling. The spin-orbit Hamiltonian matrix elements are calculated separately, as described in Sec. IV D.

Referring to Eq. (13) for matrix elements of one electron operators with respect to the 11 electron determinants $|i\rangle$ and $|j\rangle$,

$$\langle i | H^{\text{bonding}} | j \rangle = -\langle \text{hole}_j | H^{\text{bonding}} | \text{hole}_i \rangle \quad (i \neq j),$$

$$\langle i | H^{\text{bonding}} | i \rangle = \langle I_2^{2-} | H^{\text{bonding}} | I_2^{2-} \rangle - \langle \text{hole}_i | H^{\text{bonding}} | \text{hole}_i \rangle, \quad (16)$$

where determinant $|i\rangle$ has a hole in molecular spin-orbital $|\text{hole}_i\rangle$.

H^{bonding} is totally symmetric in the $D_{\infty h}$ point group, and no two of the 12 molecular spin-orbitals [Eq. (11)] have both the same spin and the same spatial point group symmetry, so all the off-diagonal matrix elements are zero. This greatly reduces the number of parameters required to describe bonding in I_2^- . The 11 electron functions $|i\rangle$ are the electronic eigenfunctions of H^{bonding} with Born-Oppenheimer energies E_i ,

$$E_i = \langle i | H^{\text{bonding}} | i \rangle. \quad (17)$$

Comparison of Eqs. (16) and (17) shows that each surface E_i is described by just two integrals, $\langle I_2^{2-} | H^{\text{bonding}} | I_2^{2-} \rangle$ and $\langle \text{hole}_i | H^{\text{bonding}} | \text{hole}_i \rangle$. We now describe a procedure for fitting the integrals either to *ab initio* or to experimental potential energy surfaces.

The many-electron matrix element $\langle I_2^{2-} | H^{\text{bonding}} | I_2^{2-} \rangle$ is the same for all diagonal elements of the 12×12 Hamiltonian matrix, so it merely shifts the origin of the energy and has no effect on the relative energies of the 12 states at a particular bond length R . In the following, we first consider the energies relative to the ground state, which depend only on the one electron integrals $\langle \text{hole}_i | H^{\text{bonding}} | \text{hole}_i \rangle$, and then add a single (R -dependent) correction term to all 12 diagonal elements to reproduce the absolute energies.

It is common practice to parametrize the molecular orbital integrals ($\langle \text{hole}_i | H^{\text{bonding}} | \text{hole}_j \rangle$) in the atomic orbital basis, because it achieves a partitioning of the energy into two center chemical bonding energies and one center atomic en-

ergies. Each diagonal one electron matrix element over molecular orbitals can be expanded in the *molecule fixed Cartesian atomic orbital basis* via Eq. (11),

$$\langle \text{hole}_{i,u/g} | H^{\text{bonding}} | \text{hole}_{i,u/g} \rangle = \frac{\langle A O_{A,i} | H^{\text{bonding}} | A O_{A,i} \rangle + \langle A O_{B,i} | H^{\text{bonding}} | A O_{B,i} \rangle \pm 2 \langle A O_{A,i} | H^{\text{bonding}} | A O_{B,i} \rangle}{2(1 \pm \langle A O_{A,i} | A O_{B,i} \rangle)}. \quad (18)$$

Because H^{bonding} is only a function of the spatial coordinates, the matrix elements are independent of spin.

I_2^- is a homonuclear diatomic, so the two one-center atomic orbital integrals are equal by symmetry. For the purpose of calculating the relative energies of the pair of determinants $|i,u\rangle$ and $|i,g\rangle$ ($i = \Sigma^+, \Pi_x, \Pi_y$) at a particular R we are free to choose the origin of energy such that the one-center integrals are zero. Defining the bonding parameter β_i and the overlap S_i ,

$$\beta_i(R) = \langle A O_{A,i} | H^{\text{bonding}} | A O_{B,i} \rangle,$$

$$S_i(R) = \langle A O_{A,i} | A O_{B,i} \rangle$$

and solving Eqs. (16), (17), and (18) for β_i in terms of the Born–Oppenheimer energies of states $|i,u\rangle$ and $|i,g\rangle$ one obtains,

$$\beta_\Sigma = \frac{1 - S_\Sigma^2}{2} (E_{2\Sigma_u^+} - E_{2\Sigma_g^+}), \quad (19a)$$

$$\beta_\Pi = \frac{1 - S_\Pi^2}{2} (E_{2\Pi_u} - E_{2\Pi_g}), \quad (19b)$$

where the equations for $i = \Pi_x$ and $i = \Pi_y$ are identical since the Π states are degenerate. If the atomic p orbitals $A O_A$ and $A O_B$ have their positive lobes oriented parallel rather than anti-parallel, S_Σ and β_Σ are negative while S_Π and β_Π are positive. The defining equation for β_Σ contains an additional factor $(1 - S_\Sigma^2)$ compared to the parametrization of $(E_{2\Sigma_u^+} - E_{2\Sigma_g^+})$ directly in the molecular orbital basis via Eqs. (16) and (17). This factor is frequently absorbed into the β 's, in which case the atomic and molecular orbital parametrizations of I_2^- are identical. We have elected to retain the $(1 - S_\Sigma^2)$ term because it does improve the fit at $R \sim R_e$. However, previous studies of Hückel theory have found that inclusion of this term does not lead to a significant improvement in the overall quality of results.²⁷

In order to specify the relative energies of the four Hund's case (a) Born–Oppenheimer surfaces ${}^2\Sigma_u^+$, ${}^2\Sigma_g^+$, ${}^2\Pi_u$, and ${}^2\Pi_g$, three bonding parameters are required. In addition to $\beta_\Sigma(R)$ and $\beta_\Pi(R)$ we define $(\alpha_\Pi - \alpha_\Sigma)(R)$,

$$(\alpha_\Pi - \alpha_\Sigma) = \frac{1}{2}(E_{2\Pi_g} + E_{2\Pi_u}) - \frac{1}{2}(E_{2\Sigma_u^+} + E_{2\Sigma_g^+})$$

$(\alpha_\Pi - \alpha_\Sigma)$ is the difference between the average Π state energy and the average Σ state energy.

The two overlap functions, $S_\Sigma(R)$ and $S_\Pi(R)$, are fitted to the overlap of the $5p_z$ and $5p_x$ orbitals of atomic iodine described in Sec. IV C. The three bonding parameters $\beta_\Sigma(R)$, $\beta_\Pi(R)$ and $(\alpha_\Pi - \alpha_\Sigma)(R)$, which completely specify the energies of the excited states of I_2^- relative to the ground state for a particular R , are fitted to the Σ and Π Hund's case (a) potential energy surfaces. In order to specify absolute energies, the one-dimensional ground state (${}^2\Sigma_u^+$) potential energy surface for H^{bonding} is also required. An advantage of choosing the bonding parameters to describe relative energies rather than absolute energies is that, for $R \geq R_e$, β_Σ , β_Π , $(\alpha_\Pi - \alpha_\Sigma)$, S_Σ , and S_Π are each well described by a single exponential in R . In contrast, fitting the ground state energy requires a sum of Morse potential terms.

Fitting the bonding parameters to *ab initio* potential energy surfaces which omit spin–orbit coupling [Eq. (19)] is straightforward. Unfortunately no high quality *ab initio* potential energy surfaces for the ground and excited states of I_2^- have yet been published. The best available surfaces are the six experimentally derived surfaces of Chen and Wentworth,¹⁸ which include the effects of spin–orbit coupling. In order to fit the bonding parameters to these potential energy surfaces, the explicit Hamiltonian matrix including spin–orbit coupling is required.

2. The Hamiltonian matrix for $I_2(\text{CO}_2)_n$

The 12×12 Hamiltonian matrix which describes the six doubly degenerate states of $I_2(\text{CO}_2)_n$ is most conveniently expressed as a sum of four terms,

$$\mathbf{H} = \mathbf{H}^{\text{bonding}} + \mathbf{H}^{\text{so}} + \mathbf{H}^{\text{CO}_2} + E^{\text{absolute}}(R)\mathbf{I}. \quad (20)$$

Here H^{bonding} represents the $I \cdots I$ bonding interaction in I_2^- omitting spin–orbit coupling, H^{so} describes the spin–orbit interaction and H^{CO_2} describes the $I_2^- \leftrightarrow (\text{CO}_2)_n$ interaction. The Hamiltonian matrix ($H^{\text{bonding}} + H^{\text{so}}$) reproduces the energies of the excited states of I_2^- relative to the ground state at a particular R , and $E^{\text{absolute}}(R)$ is added to the 12 diagonal matrix elements to reproduce the experimentally determined ground state energy ($E_{2\Sigma_u^+}$) of isolated I_2^- .

The ordering of the 11-electron basis functions in the Hamiltonian matrix is, $\{\Sigma_u^+, \Sigma_g^+, \Pi_{x,g}, \Pi_{y,g}, \Pi_{x,u}, \Pi_{y,u}\}$,

followed by the six basis functions with β spin ($\bar{\Sigma}_u^+$ etc.) in the same order. Only H^{SO} has off-diagonal matrix elements connecting the α spin and β spin blocks. H^{bonding} , H^{CO_2} , and $(E^{\text{absolute}}(R)\mathbf{I})$ each consist of two identical 6×6 blocks, one for each spin. For $I_2^-(\text{CO}_2)_n$, the 6×6 matrix H^{CO_2} is calculated numerically as described in Sec. IV D. The one-electron integrals, initially calculated in the atomic orbital basis, are

converted to the 11-electron basis using the transformations defined by Eqs. (8), (11), and (13). The numerical integration is by far the most computationally demanding step in the construction of \mathbf{H} . Real basis functions ($\Pi_{x/y}$) are chosen in favor of complex angular momentum eigenfunctions ($\Pi_x \pm i\Pi_y$) to minimize the number of computations.

H^{bonding} is diagonal in this basis,

$$H^{\text{bonding}} = \begin{array}{c} \begin{array}{cccccc} \Sigma_u^+ & \Sigma_g^+ & \Pi_{u,g} & \Pi_{y,g} & \Pi_{u,u} & \Pi_{y,u} \\ \Sigma_u^+ & 0 & & & & \\ \Sigma_g^+ & \begin{pmatrix} E_{\Sigma_g^+ -} \\ E_{\Sigma_u^+} \end{pmatrix} & & & & \\ \Pi_{u,g} & & \begin{pmatrix} E_{\Pi_{u,g} -} \\ E_{\Sigma_u^+} \end{pmatrix} & & & \\ \Pi_{y,g} & & & \begin{pmatrix} E_{\Pi_{y,g} -} \\ E_{\Sigma_u^+} \end{pmatrix} & & \\ \Pi_{u,u} & & & & \begin{pmatrix} E_{\Pi_{u,u} -} \\ E_{\Sigma_u^+} \end{pmatrix} & \\ \Pi_{y,u} & & & & & \begin{pmatrix} E_{\Pi_{y,u} -} \\ E_{\Sigma_u^+} \end{pmatrix} \end{array} \end{array} \quad (21)$$

where the energies relative to the ground state, $(E_i - E_{\Sigma_u^+})$, are expressed in terms of the bonding parameters β_{Σ} , β_{Π} , and $(\alpha_{\Pi} - \alpha_{\Sigma})$ and the atomic orbital overlaps S_{Σ} and S_{Π} ,

$$E_{\Sigma_g^+}(R) - E_{\Sigma_u^+}(R) = -\frac{2\beta_{\Sigma}(R)}{1 - S_{\Sigma}^2(R)},$$

$$E_{\Pi_g}(R) - E_{\Sigma_u^+}(R) = \frac{1}{2}(E_{\Sigma_g^+} - E_{\Sigma_u^+}) + (\alpha_{\Pi} - \alpha_{\Sigma})(R) - \frac{\beta_{\Pi}(R)}{1 - S_{\Pi}^2(R)},$$

$$E_{\Pi_u}(R) - E_{\Sigma_u^+}(R) = (E_{\Pi_g} - E_{\Sigma_u^+}) + \frac{2\beta_{\Pi}(R)}{1 - S_{\Pi}^2(R)}.$$

The spin-orbit matrix is constructed from the matrix elements in the atomic orbital basis (Sec. IV D), using the basis transformations defined by Eqs. (8), (11), and (13). For the special case of parallel space-fixed and molecule-fixed axes ($\theta = \phi = 0$),

$$2H^{SO} = \begin{array}{c} \begin{array}{cccccccccccc} \Sigma_u^+ & \Sigma_g^+ & \Pi_{u,g} & \Pi_{y,g} & \Pi_{u,u} & \Pi_{y,u} & \Sigma_u^+ & \Sigma_g^+ & \Pi_{u,g} & \Pi_{y,g} & \Pi_{u,u} & \Pi_{y,u} \\ \Sigma_u^+ & 0 & & & & & & & & & \frac{\zeta}{2} & i\frac{\zeta}{2} \\ \Sigma_g^+ & & 0 & & & & & & \frac{\zeta}{2} & i\frac{\zeta}{2} & & \\ \Pi_{u,g} & & & 0 & -i\frac{\zeta}{2} & & & & -\frac{\zeta}{2} & & & \\ \Pi_{y,g} & & & i\frac{\zeta}{2} & 0 & & & & -i\frac{\zeta}{2} & & & \\ \Pi_{u,u} & & & & & 0 & -i\frac{\zeta}{2} & -\frac{\zeta}{2} & & & & \\ \Pi_{y,u} & & & & & i\frac{\zeta}{2} & 0 & -i\frac{\zeta}{2} & & & & \\ \Sigma_u^+ & & & & & & -\frac{\zeta}{2} & i\frac{\zeta}{2} & 0 & & & \\ \Sigma_g^+ & & & & & & & & & 0 & & \\ \Pi_{u,g} & & & & & & -\frac{\zeta}{2} & i\frac{\zeta}{2} & & & & \\ \Pi_{y,g} & & & & & & \frac{\zeta}{2} & -i\frac{\zeta}{2} & & & 0 & i\frac{\zeta}{2} \\ \Pi_{u,u} & & & & & & -i\frac{\zeta}{2} & & & & -i\frac{\zeta}{2} & 0 \\ \Pi_{y,u} & & & & & & \frac{\zeta}{2} & & & & 0 & i\frac{\zeta}{2} \\ \Sigma_u^+ & & & & & & & & & & & & \\ \Sigma_g^+ & & & & & & & & & & & & \\ \Pi_{u,g} & & & & & & & & & & & & \\ \Pi_{y,g} & & & & & & & & & & & & \\ \Pi_{u,u} & & & & & & & & & & & & \\ \Pi_{y,u} & & & & & & & & & & & & \end{array} \end{array} \quad (22)$$

where

$$A = (1 + S_{\Pi}), \quad B = (1 - S_{\Pi}),$$

$$C = \sqrt{(1 + S_{\Sigma})(1 + S_{\Pi})}, \quad D = \sqrt{(1 - S_{\Sigma})(1 - S_{\Pi})}$$

and ζ , the spin-orbit splitting parameter for atomic iodine, is 5068 cm⁻¹.⁴⁸

The correction term $E^{\text{absolute}}(R)$ is the difference between the experimentally derived ground state energy ($E_{2\Sigma_u^+}$) of isolated I₂⁻ and the lowest eigenvalue $E_0(R)$ of ($H^{\text{bonding}} + H^{\text{so}}$),

$$E^{\text{absolute}}(R) = E_{2\Sigma_u^+}(R) - E_0(R).$$

To determine $E_0(R)$, we note that the 12×12 Hamiltonian for ($H^{\text{bonding}} + H^{\text{so}}$) is block diagonal owing to the point group symmetry of isolated I₂⁻, and the lowest eigenvalue can be obtained from the 3×3 block spanned by the basis functions Σ_u^+ , $\bar{\Pi}_{x,u}$, and $\bar{\Pi}_{y,u}$. The 3×3 block can be further reduced to a 2×2 ($\Omega=1/2$) block and a 1×1 ($\Omega=-3/2$) block, where Ω is the projection of (spin+electronic) angular momentum on the molecular axis, by taking the linear combinations

$$\bar{\Pi}_{\pm,u} = \bar{\Pi}_{x,u} \pm i\bar{\Pi}_{y,u}.$$

The experimentally determined ground state has $\Omega=1/2$, so $E_0(R)$ is the lower eigenvalue of the 2×2 matrix,

$$\begin{pmatrix} 0 & -\zeta/\sqrt{(1+S_{\Sigma})(1+S_{\Pi})} \\ -\zeta/\sqrt{(1+S_{\Sigma})(1+S_{\Pi})} & (E_{\Pi_u} - E_{\Sigma_u^+}) \end{pmatrix}.$$

Although time reversal symmetry causes the 12 eigenvalues of \mathbf{H} to occur as six degenerate pairs, this symmetry operation cannot be used to block diagonalize the Hamiltonian matrix in the usual way because it is not a unitary operator.⁴¹⁻⁴³ Time reversal does reduce the number of independent matrix elements in \mathbf{H} , but in the absence of a simple block diagonalization we elect to diagonalize the full 12×12 matrix via standard methods. This is feasible even for molecular dynamics simulations where \mathbf{H} must be diagonalized for approximately 10⁵ different geometries of I₂⁻(CO₂)_n.

3. The Hamiltonian matrix for I₂⁻ in a uniform field

For the special case of I₂⁻ in a uniform electric field parallel to the molecular axis, Ω is a good quantum number and \mathbf{H} can be reduced to two identical 6×6 blocks.

In order to block diagonalize \mathbf{H} , the basis functions $\{\Pi_x, \Pi_y\}$ are replaced with $\Pi_{\pm} = \Pi_x \pm i\Pi_y$, which are eigenfunctions of \hat{j}_z , the molecule fixed projection of the (spin+electronic) angular momentum. The matrix elements of the electric field operator ($H^{\text{field}} = F\hat{z}$) in the atomic orbital basis are either $\pm FR/2$ or 0 (Sec. IV D), and they are readily transformed to the 11-electron basis using Eqs. (8), (11), and (13). Since the field is aligned parallel to the molecular axis, there is no need to distinguish between molecule and space fixed axes, and the Euler angles relating them can be set to zero provided I₂⁻ does not rotate. The total Hamiltonian for I₂⁻ in a uniform field is obtained by replacing H^{CO_2} with H^{field} in Eq. (20),

$$\mathbf{H} = H^{\text{bonding}} + H^{\text{so}} + H^{\text{field}} + E^{\text{absolute}}(R)\mathbf{I}. \quad (23)$$

E^{absolute} is the same as for I₂⁻(CO₂)_n, and

$$H^{\text{bonding}} + H^{\text{so}} + H^{\text{field}} =$$

	Σ_u^+	$\bar{\Pi}_{+,u}$	Σ_g^+	$\bar{\Pi}_{+,g}$	$\Pi_{+,g}$	$\Pi_{+,u}$
Σ_u^+	0	$-\zeta$	$-FR$			
$\bar{\Pi}_{+,u}$	$-\zeta$	$\begin{pmatrix} E_{\Pi_u} - E_{\Sigma_u^+} \\ +\zeta \\ +\lambda \end{pmatrix}$		$-F_{\Pi}$		
Σ_g^+	$-FR$		$\begin{pmatrix} E_{\Sigma_g^+} - E_{\Sigma_u^+} \\ \\ \end{pmatrix}$	$-\zeta$		
$\bar{\Pi}_{+,g}$		$-F_{\Pi}$	$-\zeta$	$\begin{pmatrix} E_{\Pi_g} - E_{\Sigma_u^+} \\ +\zeta \\ +\beta \end{pmatrix}$		
$\Pi_{+,g}$				$\begin{pmatrix} E_{\Pi_g} - E_{\Sigma_u^+} \\ -\zeta \\ -\beta \end{pmatrix}$	$-F_{\Pi}$	
$\Pi_{+,u}$					$-F_{\Pi}$	$\begin{pmatrix} E_{\Pi_u} - E_{\Sigma_u^+} \\ -\zeta \\ -\lambda \end{pmatrix}$

(24)

where

$$A = 2(1 + S_{\Pi}), \quad B = 2(1 - S_{\Pi}),$$

$$C = \sqrt{2(1 + S_{\Sigma})(1 + S_{\Pi})}, \quad D = \sqrt{2(1 - S_{\Sigma})(1 - S_{\Pi})},$$

$$F_{\Sigma} = FR/(2\sqrt{1 - S_{\Sigma}^2}), \quad F_{\Pi} = FR/(2\sqrt{1 - S_{\Pi}^2}),$$

and ζ and the E_i 's are the same as for $I_2^-(CO_2)_n$. Construction of the Hamiltonian matrix is trivial, requiring only the value of the electric field in addition to the bonding and overlap parameters.

If the electric field has a component perpendicular to the molecular axis, as will generally be the case when the field is nonuniform, then Ω is no longer a good quantum number and field dependent matrix elements couple the 4×4 ($\Omega = 1/2$) block to the 2×2 ($\Omega = 3/2$) block. The size of the largest block in the Hamiltonian matrix for I_2^- surrounded by charge distributions of various symmetries is summarized in Table II.

4. Fitting procedure for the bonding parameters

A major benefit of setting up the Hamiltonian matrix in this fashion is that the three parameters β_{Σ} , β_{Π} , and

$(\alpha_{\Pi} - \alpha_{\Sigma})$ can be fitted one at a time, eliminating the instabilities associated with multidimensional fitting. This applies even if the parameters are fitted to experimentally derived potential energy surfaces, as demonstrated below. In practice we have obtained the atomic orbital overlaps S_{Σ} and S_{Π} using the $5p$ valence atomic orbitals for iodine due to Dolg²² and the radial potential energy function for I^- via an SCF¹⁹ calculation with the same basis set. The three bonding parameters were fitted to the six experimentally derived Chen–Wentworth potential energy surfaces¹⁸ and $E_{2\Sigma_{u,1/2}^+}$ was taken to be the ground state Chen–Wentworth potential energy surface ($^2\Sigma_{u,1/2}^+$). Since there are only three parameters to fit but six potential energy surfaces, the fit can be performed in several ways. The easiest is to set the trace of \mathbf{H} equal to the sum of the experimental energies. Since at zero field the Hamiltonian [Eq. (24)] consists of two 2×2 blocks and two 1-element blocks, taking the trace gives four equations (of which only three are independent). Solving these four linear equations for the three unknowns one obtains,

$$\beta_{\Pi}(R) = \frac{1}{2} (1 - S_{\Pi}^2(R)) \left\{ E_{2\Pi_{u,3/2}}(R) - E_{2\Pi_{g,3/2}}(R) - \frac{\zeta S_{\Pi}(R)}{1 - S_{\Pi}^2(R)} \right\}, \quad (25a)$$

$$\beta_{\Sigma}(R) = \frac{1}{2} (1 - S_{\Sigma}^2(R)) \left\{ (E_{2\Sigma_{u,1/2}^+}(R) - E_{2\Sigma_{g,1/2}^+}(R)) + (E_{2\Pi_{u,1/2}}(R) - E_{2\Pi_{g,1/2}}(R)) - (E_{2\Pi_{u,3/2}}(R) - E_{2\Pi_{g,3/2}}(R)) + \frac{2\zeta S_{\Pi}(R)}{1 - S_{\Pi}^2(R)} \right\}, \quad (25b)$$

$$(\alpha_{\Pi} - \alpha_{\Sigma})(R) = \frac{1}{2} \left\{ 2(E_{2\Pi_{u,3/2}}(R) + E_{2\Pi_{g,3/2}}(R)) + \frac{3\zeta}{1 - S_{\Pi}^2(R)} - (E_{2\Pi_{u,1/2}}(R) + E_{2\Pi_{g,1/2}}(R) + E_{2\Sigma_{u,1/2}^+}(R) + E_{2\Sigma_{g,1/2}^+}(R)) \right\}.$$

The $^2\Pi_{u,1/2}$ and $^2\Sigma_{g,1/2}^+$ states are not so well determined experimentally,¹⁸ so it is desirable to eliminate them from the fitting equations. This can be achieved using the two addi-

tional independent equations which result from setting the determinant of each symmetry block of \mathbf{H} equal to the product of the corresponding experimental energies. These two additional equations are quadratic in the energy, and the algebra is somewhat more complicated than for the linear case, so a symbolic manipulation package⁴⁹ was used to solve the equations and perform the fit.

To minimize the number of fitted variables the same exponent was used for S_{Π} and β_{Π} when fitting these two exponential functions to the experimental potential energy surfaces and the *ab initio* overlap, and similarly for S_{Σ} and β_{Σ} . This approach is quite common in Hückel type calculations, despite the fact that the true exponents are generally substantially different, because the results are usually insensitive to the overlap function.²⁷ The exponent is chosen to provide an accurate fit for β and a relatively inaccurate fit for S . Because the defining equation for each β parameter (25a) and (25b) is dependent on the corresponding overlap function, β and S must be fitted simultaneously. However, the coupling is very weak so the iterative fitting procedure converges rapidly. The fitted parameters are listed in Table III. The empirical $I_2^- \leftrightarrow CO_2$ short range repulsive potential and the point

TABLE II. Size of the largest block in the Born–Oppenheimer Hamiltonian matrix for I_2^- subject to external electrostatic potentials of various symmetries.

Symmetry	Biggest block in Hamiltonian ^a
$D_{\infty h}$	2
$C_{\infty v}$	4
C_s	12
C_1	12

^aEven if the system has no point symmetry, the 12 eigenvalues occur as six degenerate pairs, owing to the enduring time-reversal symmetry (Sec. IV A). Because time-reversal is an *antilinear* operator, the representation matrices for the group containing the time reversal operator are not homomorphic to the corresponding operators. As a consequence, time-reversal cannot be used to block diagonalize the Hamiltonian matrix. However, for molecules such as Cl_2^- where spin–orbit coupling can be neglected, the Hamiltonian can be reduced at least to two 6×6 blocks, one with basis functions having α spin and one with β spin.

TABLE III. Bonding parameters for I_2^- . The parameters are defined in Sec. IV E. The energy of the ground electronic state is taken to be the experimentally derived Chen–Wentworth (Ref. 18) ${}^2\Sigma_{u,1/2}^+$ potential energy surface [Fig. 1(a)]. The iodine atomic spin–orbit splitting parameter $\zeta=5068$ cm^{-1} (Ref. 48). (Units: Bohr and eV.)

Parameter	Value
S_{Π}	$39.8 \exp(-0.901R)$
β_{Π}	$2.63 \times S_{\Pi}$
S_{Σ}	$-7.17 \exp(-0.530R)$
β_{Σ}	$3.49 \times S_{\Sigma}$
$(\alpha_{\Pi} - \alpha_{\Sigma})$	$19.6 \times \exp(-0.506R)$

charges which describe the multipoles of CO_2 are described in the Appendix. While they are required for molecular dynamics simulations of $I_2^-(\text{CO}_2)_n$, they are not needed to describe I_2^- in a uniform electric field.

5. Accuracy of the fit

The six states produced from the model Hamiltonian [Eq. (24)] are compared with the corresponding Chen–Wentworth potential energy surfaces in Fig. 1(a). For the four fitted surfaces, the main discrepancy in the fit occurs in the region of the short range repulsive wall. This is to be expected because many highly excited electronic configurations mix strongly with the six lowest energy configurations in this region, so a six configuration description of the wave function is inadequate. This is not regarded as a serious short coming because many properties of interest are expected to be insensitive to the precise shape of the short range part of the potential. (For example, very little surface hopping can occur at short range because the surfaces are too far apart.) The two upper electronic states, which were not used in the fitting procedure, are not so accurately reproduced by the model. In particular, the model surfaces exhibit a shallow minimum (~ 0.09 eV) whereas the Chen–Wentworth potentials are purely repulsive. One of these states, ${}^2\Sigma_{g,1/2}^+$, is described by two Hund’s case (a) basis functions (Σ_g^+ and $\overline{\Pi}_{+,g}$) which are brought into resonance by spin–orbit coupling. As a result of this resonance the model potential is very sensitive to the choice of parameters and a moderate error is to be expected. The ${}^2\Pi_{g,1/2}$ state is similarly affected. In contrast, the well depth for the ${}^2\Pi_{u,1/2}$ state is relatively insensitive to changes in the fitted parameters. The well is produced by spin–orbit mixing of the antibonding $\overline{\Pi}_{+,u}$ and bonding Σ_u^+ Hund’s case (a) configurations. It is difficult to distinguish between fitting errors intrinsic to the model and fitting errors related to inaccuracies in the experimental potential energy surfaces since the upper two states are not uniquely determined experimentally. However, the excellent fit to crude *ab initio* calculations (discussed in Sec. III) lends credence to the model.

F. Application of the model Hamiltonian: Nonradiative electronic transitions in $I_2^-(\text{CO}_2)_n$

Experimental studies of electronically excited I_2^- in a cluster of CO_2 molecules^{3,5} suggest that the CO_2 solvent induces a rapid (~ 2 ps) nonradiative electronic and vibrational relaxation of I_2^- . Experiments on I_2^- in liquid ethanol and

water¹¹ have concluded that the *electronic* relaxation occurs in less than 300 fs. While molecular dynamics studies⁵ have confirmed that rapid vibrational relaxation of I_2^- does occur, the electronic relaxation was assumed to happen with unit probability at a bond length of 12 Bohr. The mechanism for the nonradiative electronic decay of I_2^- remains a subject of debate and we are extending the molecular dynamics simulations of Papanikolas *et al.*⁵ to include these transitions via the semiclassical surface hopping method of Tully.⁵⁰

In this section we outline the calculation of surface-hopping properties of the electronic wave function required for the molecular dynamics simulation. Results of the simulations and details of the molecular dynamics algorithm will be reported in the future.⁵¹

1. Summary of surface hopping theory

The total Hamiltonian for the cluster can be written as

$$\mathbf{H}_{\text{cluster}} = \hbar^2 \mathbf{T}_X + \mathbf{H}(\mathbf{r}; \mathbf{X}) + \mathbf{V}_{\text{CO}_2, \text{CO}_2}(\mathbf{X}),$$

where \mathbf{r} represents the electronic coordinate, \mathbf{X} the nuclear coordinates, $\hbar^2 \mathbf{T}_X$ the kinetic energy of the nuclei, \mathbf{H} the electronic Hamiltonian [Eq. (20)], and $\mathbf{V}_{\text{CO}_2, \text{CO}_2}$ the $\text{CO}_2 \leftrightarrow \text{CO}_2$ interaction potential.

Each CO_2 molecule in the $I_2^-(\text{CO}_2)_n$ cluster is modeled as a rigid body^{26,17} and its quadrupole and hexadecapole moments fitted to five point charges as described in the Appendix. $\mathbf{V}_{\text{CO}_2, \text{CO}_2}$ is approximated as a sum of pairwise interaction potentials.²⁶ All coordinates refer to axes parallel to space fixed axes with origin at the nuclear center of mass of the cluster. \mathbf{X} is assumed to be a function of time, with the trajectory to be determined by numerical integration of the nuclear equations of motion. The time-dependent wave function for the electronic coordinate is expanded in the basis of the six doubly degenerate eigenfunctions of \mathbf{H} , ϕ_l , with eigenvalues $\epsilon_l(\mathbf{X})$,

$$\Psi(\mathbf{r}, \mathbf{X}, t) = \sum_{l=1}^{12} c_l(t) \phi_l(\mathbf{r}; \mathbf{X}). \quad (26)$$

The complex coefficients $c_l(t)$ are evaluated by substituting (26) into the time-dependent Schrödinger equation,

$$[\hbar^2 \mathbf{T}_X + \mathbf{H} + \mathbf{V}_{\text{CO}_2, \text{CO}_2}] \Psi = i \hbar \frac{d\Psi}{dt}.$$

Multiplying on the left by $\phi_m(\mathbf{r}; \mathbf{X})$, integrating over \mathbf{r} and making use of the chain-rule for d/dt ,

$$\left\langle \phi_m \left| \frac{d}{dt} \phi_l \right. \right\rangle = \dot{\mathbf{X}} \cdot \langle \phi_m | \nabla_{\mathbf{X}} \phi_l \rangle$$

one obtains an equation for the evolution of the coefficients c ,

$$i \hbar \dot{c}_m = c_m (\epsilon_m + \mathbf{V}_{\text{CO}_2, \text{CO}_2}) + \sum_l c_l \left\{ \dot{\mathbf{X}} \cdot \langle \phi_m | -i \hbar \nabla_{\mathbf{X}} | \phi_l \rangle + \langle \phi_m | \hbar^2 \mathbf{T}_X | \phi_l \rangle \right\}. \quad (27)$$

The term $\nabla_{\text{CO}_2, \text{CO}_2}$ does not affect the relative phases of the c 's and can be omitted, provided the CO_2 molecules are assumed to be nonpolarizable. If the term involving $\hbar^2 \mathbf{T}_X$ on the right-hand side of Eq. (27) is omitted, one obtains the classical path equation⁵² used in Tully's surface hopping theory. At each time step in a molecular dynamics simulation the coupled differential equations [Eq. (27)] neglecting the $\hbar^2 \mathbf{T}_X$ term can be integrated numerically to obtain the amplitudes $c_l(t)$ of each electronic state. Electronic surface hoppings between states ϕ_l and ϕ_m occur with a probability proportional to the off-diagonal elements of the term $\mathbf{X} \cdot \langle \phi_m | -i\hbar \nabla_{\mathbf{X}} | \phi_l \rangle$, and the forces on the nuclei are determined from the gradient of one of the six potential energy surfaces ϵ_l . The Tully surface hopping algorithm prescribes which forces should be used at each time step.

Since $\hbar^2 \mathbf{T}_X$ is neglected in most implementations of surface hopping theory, Λ doubling (electronic-nuclear rotation coupling) and other nonadiabatic effects are omitted from the energy and forces. Nevertheless, surface hopping induced by electronic-nuclear rotation coupling (Coriolis coupling) or any other nonadiabatic coupling is included, because $-i\hbar \nabla_{\mathbf{X}}$ spans all $3N$ components of nuclear momenta, including rotation of the entire system. The validity of the classical path method for rovibronic transitions has been tested by Parlant and Alexander⁵³ who found good agreement between quantum and classical path rovibronic transition probabilities for the collision of helium with $\text{CN}(^2\Pi_{1/2}$ and $^2\Pi_{3/2})$. Tully⁵⁰ has noted that the chief problem with the classical path method lies in reproducing interference effects stemming from the wave function for nuclear motion, though it is believed that such effects are most important in systems with few degrees of freedom.

While the gradient operator $\nabla_{\mathbf{X}}$ refers to the $3N$ space fixed Cartesian coordinates of the N nuclei, most applications to date have used translational and rotational invariance to reduce the number of derivatives to be evaluated from $3N$ to $3N-6$. For a system containing three atoms this reduces the number of derivatives to be computed at each time step from nine to three.^{54,55} For larger systems the use of internal coordinates complicates the integration of Newton's equations of motion for the nuclei and it is easier to use all $3N$ coordinates. We have used all $3N$ space fixed cartesian derivatives for molecular dynamics studies of I_2^- in a cluster of CO_2 molecules, while for studies of isolated I_2^- in an electric field the independent coordinates were taken to be the I_2^- bond length and the field strength.

2. Calculation of forces and surface hopping matrix elements

For simplicity we set $\hbar=1$ in this section. At each time step in the molecular dynamics simulation the 12 electronic eigenfunctions of the cluster, ϕ , are expanded in the basis of 11-electron determinants $|i\rangle$,

$$\phi(\mathbf{r}; \mathbf{X}) = \Gamma^t(\mathbf{X}) |i(\mathbf{r}; R)\rangle, \quad (28)$$

where R is the bond length of I_2^- . The basis functions $|i\rangle$ are the eigenfunctions for isolated I_2^- omitting spin-orbit coupling [Eq. (17)]. The forces \vec{F} on the nuclei,

$$\vec{F}_l = -\nabla_{\mathbf{X}} \epsilon_l(\mathbf{X}) - \nabla_{\mathbf{X}} \nabla_{\text{CO}_2, \text{CO}_2},$$

and the surface hopping matrix elements \vec{d} ,

$$\vec{d}_{ml} = \langle \phi_m | \nabla_{\mathbf{X}} \phi_l \rangle,$$

are required at each time step. As discussed in Sec. IV D, \vec{d} is a skew-Hermitian matrix. It describes the change in the wave functions ϕ as the nuclei are displaced,

$$\nabla_{\mathbf{X}} \phi = \vec{d}' \phi. \quad (29)$$

It is well known from Rayleigh-Schrödinger perturbation theory that, if the wave function is expanded in a Taylor series in the perturbation λ ,

$$\psi(\lambda) = \psi^{(0)} + \lambda \psi^{(1)} + \dots$$

then the first-order wave function $\psi^{(1)}$ may be chosen to be orthogonal to the unperturbed wave function,

$$\langle \psi^{(0)} | \psi^{(1)} \rangle = 0.$$

This choice is equivalent to setting to zero the diagonal elements of \vec{d} and each off-diagonal element $\vec{d}_{ll'}$ coupling a degenerate pair of states $\{\phi_l, \phi_{l'}\}$,

$$\begin{pmatrix} \vec{d}_{ll} & \vec{d}_{ll'} \\ \vec{d}_{l'l} & \vec{d}_{l'l'} \end{pmatrix} = \begin{pmatrix} 0 & 0 \\ 0 & 0 \end{pmatrix}. \quad (30)$$

For $I_2^-(\text{CO}_2)_n$ the wave functions ϕ_l occur in degenerate pairs related by the time reversal operator θ ,

$$\phi_{l'} = \theta \phi_l.$$

Both \vec{F} and \vec{d} involve $\nabla_{\mathbf{X}} \phi$, which can be expanded in terms of $\nabla_{\mathbf{X}} \Gamma$ and $\nabla_{\mathbf{X}} |i\rangle$ via Eq. (28). The derivative of the C.I. coefficients, $\nabla_{\mathbf{X}} \Gamma$, can be eliminated by application of the defining equations for the eigenfunctions ϕ ,

$$\begin{aligned} \mathbf{H}\Gamma &= \mathbf{S}\Gamma\epsilon, \\ \Gamma^\dagger \mathbf{S}\Gamma &= \mathbf{I}, \end{aligned} \quad (31)$$

where

$$\begin{aligned} \epsilon_{ml} &= \epsilon_m \delta_{ml}, \\ H_{ij} &= \langle i | \mathbf{H} | j \rangle, \end{aligned}$$

and

$$S_{ij} = \langle i | j \rangle. \quad (32)$$

Denoting the matrix representation of $\nabla_{\mathbf{X}}$ in the $|i\rangle$ basis by \vec{D} ,

$$\vec{D}_{ij} = \langle i | \nabla_{\mathbf{X}} | j \rangle, \quad (33)$$

\vec{d} and $\nabla_{\mathbf{X}} \epsilon$ are evaluated using the formula,³⁸

$$\begin{aligned} [\epsilon, \vec{d}] - \nabla_{\mathbf{X}} \epsilon &= -\Gamma^\dagger (\nabla_{\mathbf{X}} \mathbf{H}) \Gamma + \frac{1}{2} [\epsilon, \Gamma^\dagger (\vec{D} - \vec{D}^\dagger) \Gamma] \\ &\quad + \frac{1}{2} [\epsilon \Gamma^\dagger (\nabla_{\mathbf{X}} \mathbf{S}) \Gamma + \Gamma^\dagger (\nabla_{\mathbf{X}} \mathbf{S}) \Gamma \epsilon], \end{aligned} \quad (34)$$

where

$$[\epsilon, \vec{d}] = \epsilon \vec{d} - \vec{d} \epsilon$$

ϵ is a diagonal matrix, so the commutator matrices $[\epsilon, \vec{d}]$ and $[\epsilon, \Gamma^\dagger (\vec{D} - \vec{D}^\dagger) \Gamma]$ are easy to evaluate and their diagonal elements are zero. Consequently, the diagonal elements of Eq. (34) determine $\nabla_{\mathbf{X}} \epsilon$ in terms of Γ , ϵ , $\nabla_{\mathbf{X}} \mathbf{S}$, and $\nabla_{\mathbf{X}} \mathbf{H}$. The

off-diagonal elements of $\nabla_{\mathbf{x}}\epsilon$ are zero, since ϵ is diagonal, and the off-diagonal elements of Eq. (34) determine $\vec{\mathbf{d}}$ in terms of $\vec{\mathbf{D}}$, Γ , ϵ , $\nabla_{\mathbf{x}}\mathbf{S}$, and $\nabla_{\mathbf{x}}\mathbf{H}$. A further simplification arises because the basis $|i\rangle$ is orthonormal so $\mathbf{S}=\mathbf{I}$ and $\nabla_{\mathbf{x}}\mathbf{S}=\mathbf{0}$.

The matrix $\nabla_{\mathbf{x}}\mathbf{H}$ is the derivative of the Hamiltonian matrix expressed in the $|i\rangle$ basis [Sec. IV E and Eqs. (20)–(22)]. \mathbf{H} contains I–I bonding terms, spin–orbit terms and $I_2^- \leftrightarrow \text{CO}_2$ interaction terms. Each I–I bonding and spin–orbit element is a simple function of the I–I bond length and is readily differentiated [Eqs. (21) and (22)]. The $I_2^- \leftrightarrow \text{CO}_2$ interaction matrix elements are each sums of one-electron nuclear attraction integrals over Cartesian (p) Gaussians, and differentiation of these integrals is a standard procedure in quantum chemistry programs which calculate the analytic gradient of the Hartree–Fock energy.

Evaluation of the matrix $\vec{\mathbf{D}}$ is detailed in Sec. IV D. Since $\nabla_{\mathbf{x}}$ is a one-electron operator, the usual rules for matrix elements of one-electron operators between determinants $|i\rangle$ have been applied. The resulting expression for $\vec{\mathbf{D}}$ involves the derivatives of the molecular orbital coefficients \mathbf{C} [Eq. (11)], the derivatives of the Euler angles (θ, ϕ) defining the orientation of I_2^- in the space fixed frame, and the derivatives of the (space fixed) atomic orbitals. The molecular orbital coefficients and Euler angles are simple functions of the coordinates of the two iodine nuclei, and are readily differentiated. Physically, the Euler angle derivatives describe Coriolis (electron–nuclear rotation) coupling in I_2^- . The derivatives of the atomic orbitals, $\langle AO_\alpha | \nabla_{\mathbf{x}} AO_\beta \rangle$, are neglected. Jepsen and Hirschfelder⁵⁶ found that the contribution of the atomic orbital derivatives to $\vec{\mathbf{d}}$ is very sensitive to the details of the wave function while Tully³⁸ and Thorsen⁵⁷ have noted that these terms can give rise to small but spurious surface hopping probabilities. The later point is easily demonstrated for an isolated hydrogen atom in the ground electronic state traveling in the Z direction. The integral $\langle 2p_z | (d/dZ) 1s \rangle$ is nonzero, so classical path theory would erroneously predict that translational motion of the isolated atom induces electronic transitions between the $1s$ and $2p_z$ states. It is thought that omission of this term is a relatively minor approximation because nonadiabatic transitions usually occur when $\epsilon_m \approx \epsilon_l$, in which case the dominant contribution to \vec{d}_{ml} [Eq. (34)] comes from $(d/dZ)\mathbf{H}$ which is multiplied by the factor $1/(\epsilon_m - \epsilon_l)$. Because the contribution of $\vec{\mathbf{D}}$ to $\vec{\mathbf{d}}$ occurs in the symmetrized form $(\vec{\mathbf{D}} - \vec{\mathbf{D}}^\dagger)$, approximations to $\vec{\mathbf{D}}$ such as the omission of the atomic orbital derivatives do not affect the skew-Hermitian character of $\vec{\mathbf{d}}$.

The phase choice for $\vec{\mathbf{d}}$ [Eq. (30)] constrains the evolution of degenerate pairs of wave functions, ϕ_l and $\phi_{l'}$, as the nuclei of the cluster move about on a potential energy surface [Eq. (29)]. In practice, a random phase is introduced at each time step when the ϕ 's are calculated by numerical diagonalization of \mathbf{H} . To derive a correction for the random phase we calculate $\nabla_{\mathbf{x}}\phi$ via Eq. (29) for the degenerate pair ϕ_l and $\phi_{l'}$, subject to the constraints on $\vec{\mathbf{d}}$ [Eq. (30)],

$$\nabla_{\mathbf{x}}\phi = \vec{d}'\phi = 0,$$

where it is understood that the equation only applies in the subspace spanned by ϕ_l and $\phi_{l'}$. ϕ can be expanded via Eq. (28) to give,

$$(\nabla_{\mathbf{x}}\Gamma^v)|i\rangle = -\Gamma^v\nabla_{\mathbf{x}}|i\rangle.$$

Integrating over $\langle j|$, taking the transpose and making use of Eqs. (32) and (33) one obtains,

$$\mathbf{S}(\nabla_{\mathbf{x}}\Gamma) = -\vec{\mathbf{D}}\Gamma.$$

If the nuclear displacement during the course of one time step is denoted by $\delta\vec{\mathbf{X}}$,

$$\delta\vec{\mathbf{X}} = \mathbf{X}(t+1) - \mathbf{X}(t)$$

then the finite difference approximation to the gradient of Γ ,

$$\delta\vec{\mathbf{X}} \cdot \nabla_{\mathbf{x}}\Gamma \approx \Gamma(t+1) - \Gamma(t)$$

can be inserted to yield,

$$\mathbf{S}[\Gamma(t+1) - \Gamma(t)] \approx -\delta\vec{\mathbf{X}} \cdot \vec{\mathbf{D}}\Gamma(t).$$

Multiplying by $\Gamma^\dagger(t+1)$ and making use of the orthonormality of the eigenvectors [Eq. (31)] a constraint condition for $\Gamma(t+1)$ is obtained,

$$\Gamma^\dagger(t)(\mathbf{S} + \delta\vec{\mathbf{X}} \cdot \vec{\mathbf{D}})\Gamma(t+1) = \mathbf{I}, \quad (35)$$

where it is understood that the equation only applies to degenerate sets of ϕ 's. The $|i\rangle$ basis is orthonormal, so $\mathbf{S}=\mathbf{I}$. \mathbf{S} has been retained in the above expressions because it is common practice to use nonorthogonal sets of valence-bond basis functions. To make the expression as symmetric as possible we use a central difference expression for $\vec{\mathbf{D}}$ at the mid-point $(t+1/2)$ of the time step, and also enforce the skew-Hermitian property of $\vec{\mathbf{D}}$,

$$\vec{\mathbf{D}}(t+1/2) \approx \frac{\frac{1}{2}[\vec{\mathbf{D}}(t) - \vec{\mathbf{D}}^\dagger(t)]}{2} + \frac{\frac{1}{2}[\vec{\mathbf{D}}(t+1) - \vec{\mathbf{D}}^\dagger(t+1)]}{2}.$$

If at time $(t+1)$ the matrix diagonalization introduces a random phase into $\phi_l(t+1)$ and $\phi_{l'}(t+1)$, represented by the 2×2 unitary matrix $\mathbf{U}(t+1)$,

$$\Gamma'(t+1) = \Gamma(t+1)\mathbf{U}(t+1).$$

Then from Eq. (35),

$$\mathbf{U}(t+1) = \Gamma^\dagger(t)(\mathbf{S} + \delta\vec{\mathbf{X}} \cdot \vec{\mathbf{D}})\Gamma'(t+1)$$

$\mathbf{U}(t+1)$ is readily calculated from the eigenvectors Γ and surface hopping matrix elements $\vec{\mathbf{D}}$ in the 11-electron basis $|i\rangle$. The phase constrained eigenvectors $\Gamma(t+1)$ are

$$\Gamma(t+1) = \Gamma'(t+1)\mathbf{U}^\dagger(t+1).$$

\mathbf{U} is only exactly unitary for an infinitesimal time step, and in practice \mathbf{U} is multiplied by a normalization factor at each time step. For a two-fold degeneracy the normalization factor is $+1/\sqrt{|\det[\mathbf{U}(t+1)]|}$. If the eigenvectors are real and non-degenerate, \mathbf{U} reduces to a phase factor of ± 1 . However, for $I_2^-(\text{CO}_2)_n$ the wave functions are complex and doubly degenerate, so \mathbf{U} is a random (complex) 2×2 unitary matrix.

V. CHARGE SWITCHING AND NONADIABATIC TRANSITIONS IN I_2^-

Molecular dynamics simulations of photodissociation of I_2^- in $I_2^-(CO_2)_n$ have found that the CO_2 cage distorts to create an appreciable potential difference between the iodine nuclei during the course of photodissociation.^{4,5,17} The forces between I_2^- and the CO_2 molecules are much stronger than for an uncharged system and the effect of the dominant coulombic interaction term on the electronic structure of I_2^- can be modeled as an applied electric field. The field strength is taken to be the potential difference between the two iodine nuclei divided by the bond length. Papanikolas *et al.* have found that fields derived in this manner from molecular dynamics simulations are typically ~ 0.003 a.u. and may be as high as 0.01 a.u. In reality the field produced by the cluster is not uniform but we expect that the polarization of I_2^- along the molecular axis will be dominated by the potential difference between the iodine nuclei, with the finer details of the potential having only a small effect.

A. I_2^- in a uniform electric field

The response of I_2^- to an electric field is complicated by spin-orbit coupling and is most easily understood by comparison with a molecule which has negligible spin-orbit coupling. Figure 1(b) shows the four potential energy surfaces for a hypothetical I_2^- molecule with no spin-orbit coupling, X_2^- , subject to an electric field F of 0.003 a.u. parallel to the molecular axis. The electric field points from nucleus X_A toward nucleus X_B , with nucleus X_A at higher potential (up-field). The surfaces were calculated using the model Hamiltonian for I_2^- [Eq. (20)], omitting the spin-orbit contribution H^{SO} [Eq. (22)]. The surfaces are typical of an ion such as H_2^+ , F_2^- , or Cl_2^- which can be represented by a one-electron p^1 or a one-hole p^5 wave function. To make the comparison concrete, the lower two surfaces correspond to the Σ and Π bonding states of a one-hole function (X_2^-), while the upper two surfaces correspond to the Σ^* and Π^* antibonding states. In the absence of spin-orbit coupling Π states consist of degenerate $\Omega=1/2$ and $\Omega=3/2$ pairs, so there are only four distinct surfaces as opposed to six for I_2^- . At long bond lengths (R) the bonding ($2p\sigma$)¹ and ($2p\pi$)¹ states converge and can be represented as $X_A^- - X_B^-$ with X_A^- at $-R/2$ and X_B^- at $+R/2$ relative to the origin at the center of mass. The potential energy relative to the center of mass at long bond lengths is simply $-FR/2$, since the charge is localized at $-R/2$. The two antibonding states correspond to $X_A - X_B^-$ with X_B^- at $+R/2$ and asymptotic energy $+FR/2$. It may seem surprising that the antibonding wave functions undergo charge localization in the "wrong" direction. However, in the one-hole picture it can readily be seen that, if the bonding state ψ is expanded in terms of identical atomic orbitals p_A and p_B on atoms A and B,

$$\psi = [\sqrt{1 - \delta^2} p_A + \delta p_B], \quad (36a)$$

then, neglecting atomic orbital overlap, the orthogonal antibonding state is

$$\psi^* = [\delta p_A - \sqrt{1 - \delta^2} p_B], \quad (36b)$$

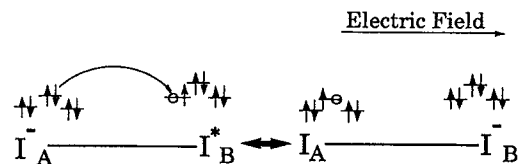


FIG. 2. Field induced resonance in I_2^- . The atomic orbitals on each atom are split by spin-orbit coupling and resonance occurs when the potential difference between the iodine nuclei due to the applied electric field = the spin-orbit splitting energy, enabling a charge transfer transition. I^* indicates iodine in the high spin-orbit energy configuration and I the low spin-orbit energy configuration. The energy origin is at the center of mass of I_2^- . A and B denote the two iodine nuclei. The hollow circle denotes a "hole."

which clearly localizes on the opposite atom as $\delta \rightarrow 0$. The "charge switching" function for X_2^- in an electric field, defined as the Mulliken charge³⁰ on atom A for a given electronic state, varies monotonically with field strength from $-1/2$ to -1 for the bonding states and $-1/2$ to 0 for the antibonding states. Because the bonding potential energy surfaces are well separated from the antibonding surfaces in the presence of an electric field we expect that nonadiabatic bonding \leftrightarrow antibonding (electron transfer) transitions will not occur.

The situation is more complicated for a molecule with spin-orbit coupling because the spin-orbit interaction [Eq. (22)] mixes bonding and anti-bonding Hund's case (a) states. Fig. 1(a) shows the potential energy surfaces for I_2^- including spin-orbit coupling at zero field while Figs. 1(c) and 1(d) show the corresponding surfaces at fields of 0.003 and 0.006 a.u. Ω , the projection of (spin+orbital) angular momentum on the molecular axis, is a good quantum number. When a field is applied there are four distinct surfaces at large R , as opposed to two for X_2^- . The four surfaces correspond to $I_A^- - I_B^-$ and $I_A^- - I_B^*$, which are bonding, and $I_A - I_B^-$ and $I_A^* - I_B^-$, which are antibonding. I^* indicates the high spin-orbit energy configuration of atomic iodine and I the low energy spin-orbit configuration. At long bond lengths a clear distinction can be made between potential energy surfaces which are similar to the Hund's case (a) bonding potential energy surfaces of Fig. 1(b) and potential energy surfaces which are similar to antibonding surfaces. In the strong field limit (0.006 a.u.) the bonding surfaces are well separated from the antibonding surfaces, in keeping with the behavior of potential energy surfaces omitting spin-orbit coupling [Fig. 1(b)]. However, the potential energy surfaces at medium field (0.003 a.u.) are very different, featuring a strong charge transfer resonance at 12 Bohr between the second and third $\Omega=1/2$ states, $I_A - I_B^-$ (anti-bonding) and $I_A^- - I_B^*$ (bonding). This resonance, illustrated in Fig. 2, occurs when the atomic spin-orbit splitting energy approximately equals the potential difference between the two iodine nuclei created by the electric field. Simulations by Papanikolas¹⁷ suggest that fields strengths of this magnitude occur in (${}^2\Pi_{g,1/2}$) photo-excited $I_2^-(CO_2)_n$ when the $I \cdots I$ bond length is in the range 9 to 12 Bohr. At weak fields the crossing occurs at very long bond lengths, precluding a charge transfer transition. As the field strength increases the distance of closest approach moves to shorter bond lengths and the crossing distance be-

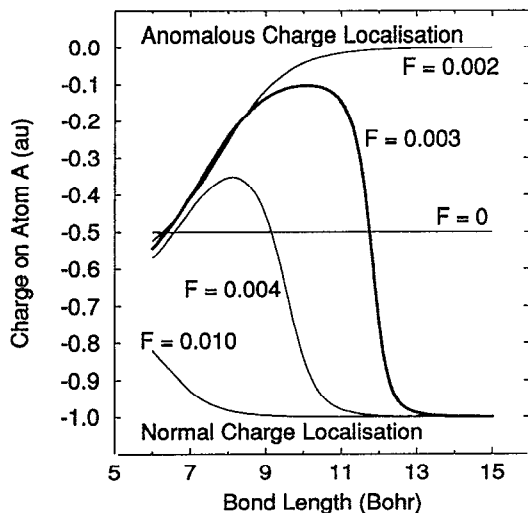


FIG. 3. Charge localization for the second $\Omega=1/2$ ($^2\Pi_{g,1/2}$) adiabatic state of I_2^- as a function of bond length and electric field (F) in a.u. The applied field points from A to B . The negative charge localizes on one iodine nucleus (A) if I_2^- dissociates in the presence of a strong electric field (≥ 0.004 a.u.) and on the other nucleus (B) in the presence of a weak electric field (≤ 0.002 a.u.). For intermediate fields the charge moves in opposite directions on either side of the avoided crossing, with the crossing occurring at ≈ 12 Bohr for a field of 0.003 a.u.

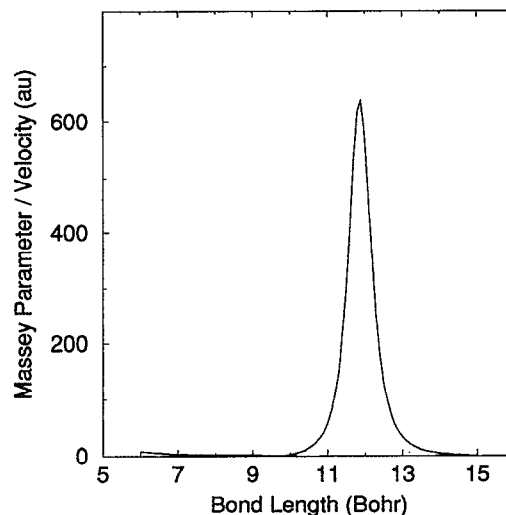


FIG. 4. Non-adiabatic transition probability for I_2^- in an electric field of 0.003 a.u. The y axis is the Massey parameter [Eq. (37)] divided by the relative velocity of the iodine nuclei. The probability of nonadiabatic transitions is closely related to the Massey parameter (see Sec. V for details).

tween the surfaces increases until the strong field limit is reached where the energy ordering of the $I_A-I_B^-$ and $I_A^-I_B^*$ configurations is reversed relative to the weak field limit for all bond lengths and the resonance is eliminated. Chemically interesting resonances occur only for field strengths in the approximate range 0.003→0.005 a.u. The field-induced avoided crossing leads to unusual charge switching functions for the excited adiabatic states and also has implications for nonadiabatic behavior.

The charge switching function for the second $\Omega=1/2$ adiabatic state, which is one of the two states involved in the resonance, is shown in Fig. 3 for several values of the electric field. At weak fields (0.002 a.u.) the negative charge localizes on the down-field atom (B) as the bond is stretched while at strong fields (0.010 a.u.) it localizes on the up-field atom (A). At a field strength of 0.003 a.u. the charge first shifts toward atom B as the bond is stretched and then, as the molecule passes adiabatically through the avoided crossing region, the character of the wave function alters suddenly and the charge shift reverses, finally localizing entirely on atom A .

The strength and location of the resonance is chiefly dependent on the magnitude of the atomic spin-orbit splitting and is quite insensitive to variation of the fitted bonding parameters. The resonance can be reproduced by a 2×2 Hamiltonian expressed in terms of the two Hund's case (c) functions [Eq. (10)] involved in the resonance. However, the algebra provides little insight beyond that to be derived from Fig. 2.

It is interesting to note that, for the second $\Omega=1/2$ adiabatic state at a field strength of 0.003 a.u., the wave function at $R \sim 7$ Bohr corresponds to the low spin-orbit energy $I_A-I_B^-$ configuration while at dissociation the wave function

is dominated by the high spin-orbit energy $I_A^-I_B^*$ configuration. One may ask under what conditions I_2^- is likely to travel *adiabatically* along this surface. Nonadiabatic electronic transitions between adiabatic states i and j are probable if the Massey parameter⁵⁸ P_{ij} is of order unity,

$$P_{ij} = \left| \frac{\hbar \dot{R} d_{ij}}{E_i - E_j} \right| \geq 1. \quad (37)$$

[E_i and E_j are the energies of the adiabatic potential energy surfaces, d_{ij} is the transition matrix element defined in Eq. (34) and \dot{R} is the relative velocity of the iodine nuclei.] Since the transition matrix element d_{ij} also varies as $1/(E_i - E_j)$ [Eq. (34)] the maximum value of the Massey parameter is an extremely sensitive function of the energy gap ($E_i - E_j$) between the surfaces. The formula requires the velocity R , and a molecular dynamics simulation of $I_2^-(CO_2)_n$ will be required to characterize its distribution. If the nuclei travel sufficiently slowly, the electronic wave function has plenty of time to adjust and the nuclei follow the Born-Oppenheimer potential energy surfaces. If the nuclei travel quickly through an avoided crossing region where the adiabatic electronic wave function varies rapidly with bond length, the electrons may not have time to relax and a nonadiabatic transition can occur. Figure 4 gives the Massey parameter divided by the nuclear velocity, $|\hbar \dot{R} d_{ij}/E_i - E_j|$, for the two adiabatic states involved in the resonance at a field of 0.003 a.u. The Massey parameter peaks at the avoided crossing (at 12 Bohr) and has a width at half the peak height of about 1 Bohr. If I_2^- has 0.3 eV of kinetic energy, probably a typical value for photodissociation experiments, one obtains $P_{23} = 0.29$ using Eq. (37). Since this is significantly less than unity, adiabatic motion linking the $I_A-I_B^-$ and $I_A^-I_B^*$ configurations is highly probable in a field of 0.003 a.u.

B. Possible mechanisms for electronic relaxation of I_2^- in a CO_2 cluster

In this section the field-dependent potential energy surfaces for I_2^- described in Sec. V A are applied to the problem of electronic relaxation of I_2^- in a cluster of n CO_2 molecules.

In the experiments of Papanikolas *et al.*,^{4,5} I_2^- in a CO_2 cluster is photoexcited by a 720 nm pump pulse from the ground $^2\Sigma_{u,1/2}^+$ electronic state to the repulsive $^2\Pi_{g,1/2}$ state. The clusters are size selected, with a maximum of 22 CO_2 molecules. Excited I_2^- dissociates promptly, with the kinetic energy being dissipated by the CO_2 molecules. A substantial proportion of the I_2^- molecules recombine and are subsequently excited with a probe pulse of the same frequency as the pump pulse. The time-resolved absorption intensity is observed to vary greatly with cluster size. Molecular dynamics simulations have demonstrated that, following recombination, the large polarizability of I_2^- in the ground electronic state leads to rapid vibrational relaxation in clusters⁵ and liquids.¹⁶ However, the mechanism by which I_2^- relaxes to the ground electronic state is still unclear.^{2-11,13,14,17}

Modeling of the time-dependent features of the absorption intensity will require molecular dynamics simulations of the cluster incorporating nonadiabatic electronic transitions. However, some clues as to likely electronic relaxation mechanisms can be deduced from the field-dependent potential energy surfaces and charge switching functions. The proposed mechanisms are merely suggestive, and we are currently examining the mechanisms and rates of electronic and vibrational relaxation via molecular dynamics simulations.⁵¹

The global minimum of the ground state potential energy surface for $I_2^-(CO_2)_n$ has been determined by Papanikolas¹⁷ for clusters containing 1 to 16 CO_2 molecules. If the solvation shell is full ($n=16$) or nearly empty ($n\leq 5$) the CO_2 molecules are distributed symmetrically about I_2^- , with the two iodine nuclei at approximately equal potential. For a half empty solvation shell the solvent prefers to localize around one iodine nucleus. The solvent induced potential difference between the nuclei is greatest for nine CO_2 molecules, corresponding to an applied field of 0.005 a.u. with 70% of the negative charge localized on the solvated atom. There are two equivalent minima, with a barrier of 0.3 eV to migration of the solvent between the minima. At long bond lengths, where $I\cdots I$ bonding effects are negligible, the minimum energy configuration is always localized, with the CO_2 molecules solvating the I^- ion.

Based on these results one might expect that photoexcited $I_2^-(CO_2)_n$ would dissociate to form $I\cdots I^-$, with the cluster solvating the I^- ion. Because $I_2^-(CO_2)_9$ is partially localized prior to photoexcitation, it would be expected to complete the localization process at shorter $I-I$ bond lengths than $I_2^-(CO_2)_{16}$. However, such an analysis ignores the effects of anomalous charge localization [Eq. (36)]. The ground $^2\Sigma_{u,1/2}^+$ and photoexcited $^2\Pi_{g,1/2}$ states of I_2^- correspond to the bonding and antibonding combinations of the atomic orbitals $p\sigma_A$ and $p\sigma_B$. During photoexcitation of $I_2^-(CO_2)_9$ to the antibonding state, the negative charge is expected to shift from the solvated iodine nucleus toward the unsolvated nucleus.⁵⁹ Although the CO_2 molecules are

strongly attracted to the negative charge, they cannot trap it to form solvated I^- , because it will localize anomalously for any asymmetric solvent configuration, at least for short to medium $I-I$ bond lengths. Anomalous charge localization is an inherently quantum effect, with the negative charge moving to the position of highest potential energy. As a consequence, antibonding states resist localization in a solvent more strongly than bonding states. The attractive force between the negative charge in the repulsive antibonding state and the CO_2 molecules retards the disintegration of I_2^- and promotes recombination, providing a rare chance to observe the spectroscopic effects of anomalous charge localization.

Previous molecular dynamics studies of the photodissociation of $I_2^-(CO_2)_n$ omitted anomalous charge switching,⁵ so estimates of the solvent induced potential difference experienced by I_2^- during photodissociation are unreliable. In the following, we consider the expected nonadiabatic behavior of dissociating I_2^- as the solvent induced potential difference is varied. Specifically, we consider three cases of different magnitudes of the potential difference occurring at medium bond lengths during the photodissociation of antibonding $^2\Pi_{g,1/2}I_2^-$. It is likely that the actual potential difference in a $I_2^-(CO_2)_n$ cluster varies significantly with the number of CO_2 molecules, so more than one case may be relevant.

1. Negligible field (e.g., a large number of CO_2 molecules, uniformly distributed about I_2^-)

In this case the symmetric cluster configuration of the antibonding state is expected to remain stable until very long bond lengths. Nonadiabatic transitions from the symmetric configuration of the excited state to the ground state seem highly probable at long bond lengths, because the two states are nearly degenerate [Fig. 1(a)]. The ground state would then be expected to localize rapidly to form solvated I^- . Alternatively, the excited state may undergo charge localization at long bond lengths, stimulated by random fluctuations of the solvent or a solvent-solute collision. Following charge localization, the solvent will be attracted toward the I^- ion by strong Coulombic forces. Owing to the long bond length, electron migration to the other iodine nucleus is unlikely prior to recombination of I_2^- . The electronic structure prior to recombination can be represented as $CO_2\cdots I^- \cdots I$, indicating that the solvent is clustered around I^- . This configuration corresponds to the ground state surface $I_A^- + I_B^-$ shown in Figs. 1(c) and 1(d). Interestingly, solvent migration may provide an alternative to charge transfer for relaxation to the ground electronic state.

2. Moderate field (e.g., three-quarters of a solvation shell of CO_2 molecules clustered mainly about one iodine nucleus)

A moderate to large solvent induced potential difference will cause localization of the negative charge at medium to short bond lengths. The avoided crossing involving the $^2\Pi_{g,1/2}$ state [Fig. 1(c)] moves to shorter bond lengths and I_2^- is more likely to pass through the crossing region adiabatically as the potential difference is increased (Sec. V A). If the crossing occurs at sufficiently long bond lengths then I_2^- is expected to dissociate to $I_A + I_B^-$, otherwise it is expected to

dissociate to $I_A^- + I_B^*$ [Fig. 1(d)]. A “moderate” potential difference is defined as one which results in the dissociation product $I_A + I_B^-$, while a “large” potential difference leads to $I_A^- + I_B^*$.

We presume that the moderate potential difference arises from an asymmetric solvent configuration clustered around iodine nucleus A. Intriguingly, this causes the antibonding ${}^2\Pi_{g,1/2}$ state to localize as $CO_2 \cdots I_A \cdots I_B^-$ at long bond lengths, with more solvent clustered around neutral iodine than around the iodide ion. This configuration is much higher in energy than the ground state configuration $CO_2 \cdots I_A^- \cdots I_B$, so a nonadiabatic electronic transition directly to the ground state is unlikely. However, the solvent is attracted to the iodide ion by strong Coulombic forces. At long $I \cdots I$ bond lengths, where charge transfer from nucleus B to nucleus A is not feasible, a net solvent migration from one iodine nucleus to the other would achieve relaxation to the ground state configuration $I_A \cdots I_B^- \cdots CO_2$.

The potential energy surfaces for $I_2^-(CO_2)_n$ can be viewed as functions of the $I-I$ bond length and a solvent coordinate. In the presence of a solvent-induced potential difference the $CO_2 \cdots I_A \cdots I_B^-$ and $CO_2 \cdots I_A^- \cdots I_B$ configurations are well separated energetically so an electronic surface hop is not possible. However, at long $I \cdots I$ bond lengths, an equivalent transition can occur via a smooth, continuous change of the classical solvent coordinate. Since the solvent migration reverses the potential difference experienced by I_2^- , the potential difference must pass through zero. Thus solvent migration for I_2^- subject to a moderate potential difference is an extension of solvent migration for I_2^- subject to a negligible potential difference. Along the seam of zero potential difference the configurations $I_A \cdots I_B^-$ and $I_A^- \cdots I_B$ are in resonance, so a concerted solvent migration and electron transfer cannot be ruled out. The solvent migration mechanisms for electronic relaxation in a negligible or moderate potential difference are illustrated in Figs. 5(a) and 5(b).

3. Large field (e.g., a half-empty solvation shell of highly polar solvent molecules clustered entirely about one iodine nucleus)

In this case the dissociation product is expected to be $CO_2 \cdots I_A^- \cdots I_B^*$, as discussed in (2). However, I^* is not observed experimentally. We can see no obvious relaxation pathway to the ground state configuration $CO_2 \cdots I_A^- \cdots I_B$. Collisional $I^* \rightarrow I$ relaxation is extremely slow in atomic iodine,⁶⁰ so we speculate that large potential differences are either transient or do not occur. The adiabatic surface appropriate for a large potential difference is nevertheless of some interest. It links the $I_A^- \cdots I_B^*$ configuration at dissociation with the $I_A^- \cdots I_B^-$ configuration at short bond lengths [Fig. 1(d)]. Thus if I_2^- were excited to the upper I^* spin-orbit manifold [Fig. 1(a)], fast relaxation to the lower manifold during recombination would be possible if the solvent induced potential difference were large. Relaxation within the lower manifold could subsequently occur if the potential difference decreased to a moderate or negligible value. There is considerable uncertainty concerning the state to which I_2^- in a CO_2 cluster is excited by the probe pulse. Previous studies⁴ assumed that the upper spin-orbit manifold was not involved

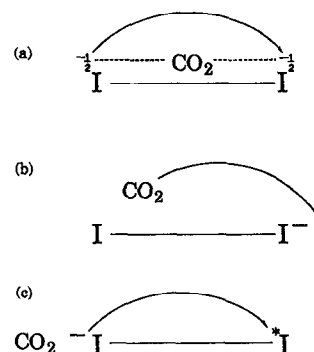


FIG. 5. Possible cluster-induced electronic relaxation mechanisms for electronically excited (${}^2\Pi_{g,1/2}$) I_2^- in a CO_2 cluster. (a) For a symmetric solvent configuration the electronically excited state (${}^2\Pi_{g,1/2}$) becomes degenerate with the ground state (${}^2\Sigma_u^+$) at long $I \cdots I$ bond lengths [Fig. 1(a)]. As the $I \cdots I$ bond length increases the delocalized electronic charge distribution $I^{-1/2} \cdots I^{-1/2}$ becomes unstable, eventually localizing randomly on one of the iodine nuclei. The solvent is strongly attracted to the resulting I^- ion and migrates towards the ground state $I \cdots I^- \cdots CO_2$ configuration. (b) The same as (a) except that the cluster is initially asymmetric. The initial configuration displays anomalous localization of the electronic charge, a feature of antibonding electronic states [Eq. (36)]. (c) Nonadiabatic relaxation from the upper I^* spin-orbit manifold of I_2^- to the lower I manifold. The CO_2 cluster provides a potential difference which brings the charge-transfer relaxation mechanism into resonance. The resonance is illustrated in Fig. 2.

because relaxation to the ground electronic state could not occur on the experimentally observed time scale (<30 ps). However, the preceding considerations of the polarizability of I_2^- cast some doubt on this assumption. The suggested mechanism for solvent induced $I^* \rightarrow I$ relaxation in I_2^- is summarized in Figs. 2 and 5(c).

The role of the two $\Omega=3/2$ states in electronic relaxation has not been considered so far. It has previously been proposed⁴ that I_2^- prepared in the second $\Omega=1/2$ state (${}^2\Pi_{g,1/2}$) inside a CO_2 cluster could undergo rapid relaxation to the lowest $\Omega=3/2$ state (${}^2\Pi_{g,3/2}$) at long bond lengths via collisions with CO_2 molecules. This mechanism seems plausible at zero field [Fig. 1(a)] because the two states are degenerate at long bond lengths. Suppose, at long $I \cdots I$ bond lengths, a CO_2 molecule approaches the iodine atom perpendicular to the I_2^- axis. It exerts a torque on the quadrupole of atomic iodine but has no effect on the spin coordinates of the electrons, leading to a rearrangement of the spin and orbital angular momenta corresponding to a $1/2 \rightarrow 3/2$ transition.⁶¹ However Fig. 1(c) demonstrates that the lowest $\Omega=3/2$ state is not degenerate with any of the excited $\Omega=1/2$ states in the presence of an electric field, so a cluster-induced potential difference will inhibit relaxation to this state.

In summary, considerations of the response of I_2^- to a solvent induced potential difference suggest that electronic relaxation may occur at long $I \cdots I$ bond lengths via a net drift of the solvent toward the I^- ion. This is in contrast to the conventional view of an electron-transfer (surface hopping) mechanism. Furthermore, rapid $I^* \rightarrow I$ relaxation may be possible if the solvent induced potential difference between the iodine nuclei exceeds the atomic spin-orbit splitting energy (0.94 eV). Unlike $I^* \rightarrow I$ relaxation, electronic relaxation by

TABLE IV. I_2^- Parameters for short range repulsive $I_2^- \leftrightarrow CO_2$ and $CO_2 \leftrightarrow CO_2$ potentials. ϵ and σ are defined in Eq. (A1) (Bohr and eV).

Parameter	Value
ϵ_{I-O}	0.0100
ϵ_{I-C}	0.009 12
σ_{I-O}	6.661
σ_{I-C}	7.015

solvent migration should be equally important in dihalide ions lacking spin-orbit coupling.

These results take into account only the gross charge drift along the I-I bond in response to an applied potential difference, ignoring the nonuniform nature of the field. While current molecular dynamics simulations include nonuniform field effects,⁵¹ they are based upon the simple one hole wave function described in Secs. II and IV. The model will be inadequate if electronic relaxation is sensitive to finer details of the wave function, such as polarization of the atomic orbitals by a collision with a CO_2 molecule. However, electronic relaxation in I_2^- is rapid,^{4,5,11} which leads us to suspect that the dominant charge-field interaction is responsible for the relaxation.

VI. CONCLUSION

A one-hole model has been devised to treat the interaction of the six lowest electronic states of I_2^- with an arbitrary distribution of point charges and multipoles. The model has been used to study the effect of a uniform electric field parallel to the molecular axis on these six states. The field perturbs the negative ion strongly, causing a resonant interaction between two states which are separated by approximately 1 eV in isolated I_2^- . Spin-orbit coupling significantly affects the response of the excited states to an electric field, with the polarizability of the ${}^2\Pi_{g,1/2}$ adiabatic state varying in both sign and magnitude as the I_2^- bond is stretched and the field strength varied.

The field-dependent potential energy surfaces have been used to investigate mechanisms for nonadiabatic relaxation of electronically excited I_2^- in a CO_2 cluster, with the effects of the CO_2 molecules approximated by a uniform electric field parallel to the molecular axis of I_2^- . While molecular dynamics simulations will be required to determine theoretical reaction rates, a study of the field-dependent potential energy surfaces suggests that more channels exist for nonadiabatic relaxation than previously suspected. In the presence of an electric field of 0.003 a.u. a state from the lower ($I_A^- - I_B^-$) spin-orbit manifold of Fig. 1(a) undergoes an avoided crossing with a state from the upper ($I_A^* - I_B^*$) manifold at approximately 12 Bohr, which suggests that $I^* \rightarrow I$ (electron-transfer) relaxation in I_2^- may be facilitated by the cluster. It is also possible that relaxation from the ${}^2\Pi_{g,1/2}$ state to the ground state at very long I-I bond lengths could proceed purely by migration of a few CO_2 molecules rather than by electron transfer. It is hoped that molecular dynamics studies⁵¹ incorporating cluster-dependent potential energy

surfaces and nonadiabatic electronic transitions will unravel the mechanisms responsible for the coherent nonadiabatic motion of I_2^- .

ACKNOWLEDGMENTS

P.E.M. wishes to thank Kazushige Yokoyama for an enlightening discussion on the effects of Λ doubling on molecules subject to strong spin-orbit coupling. This work is supported by the Air Force Office of Scientific Research.

APPENDIX: $I_2^- \leftrightarrow CO_2$ AND $CO_2 \leftrightarrow CO_2$ INTERACTION PARAMETERS

The pairwise $CO_2 \leftrightarrow CO_2$ interaction potential and the five point-charge fit to the quadrupole and hexadecapole for CO_2 required to determine the $I_2^- \leftrightarrow CO_2$ interaction Hamiltonian [Eq. (14)] were both formulated by Murthy.²⁶

The $I_2^- \leftrightarrow CO_2$ short range repulsive potential is approximated by a sum of pairwise interactions between the nuclei, each $I \leftrightarrow CO_2$ interaction being the sum of three terms of the form

$$V_{ij}(r) = 4\epsilon_{ij} \left(\frac{\sigma_{ij}}{r} \right)^{12}. \quad (A1)$$

The pairwise interaction parameters¹⁷ ϵ and σ are given in Table IV.

The geometry for CO_2 was taken from Herzberg.³⁹

- C. J. Delbecq, W. Hayes, and P. H. Yuster, *Phys. Rev.* **121**, 1043 (1961).
- J. M. Papanikolas, J. R. Gord, N. E. Levinger, D. Ray, V. Vorsa, and W. C. Lineberger, *J. Phys. Chem.* **95**, 8028 (1991).
- J. M. Papanikolas, V. Vorsa, M. E. Nadal, P. J. Campagnola, J. R. Gord, and W. C. Lineberger, *J. Chem. Phys.* **97**, 7002 (1992).
- J. M. Papanikolas, V. Vorsa, M. E. Nadal, P. J. Campagnola, H. K. Buchenau, and W. C. Lineberger, *J. Chem. Phys.* **99**, 8733 (1993).
- J. M. Papanikolas, P. J. Campagnola, V. Vorsa, M. E. Nadal, H. K. Buchenau, R. Parson, and W. C. Lineberger, in *The Chemical Dynamics and Kinetics of Small Radicals*, edited by K. Liu and A. Wagner, *Advances in Physical Chemistry*, submitted.
- U. Banin, A. Waldman, and S. Ruhman, *J. Chem. Phys.* **96**, 2416 (1992).
- U. Banin, P. Kosloff, and S. Ruhman, *Israel J. Chem.* **33**, 141 (1993).
- U. Banin and S. Ruhman, *J. Chem. Phys.* **99**, 9318 (1993).
- A. E. Johnson, N. E. Levinger, and P. F. Barbara, *J. Phys. Chem.* **96**, 7841 (1992).
- D. A. V. Kliner, J. C. Alfano, and P. F. Barbara, *J. Chem. Phys.* **98**, 5375 (1993).
- J. C. Alfano, Y. Kimura, P. K. Walhout, and P. F. Barbara, *Chem. Phys.* **175**, 147 (1993).
- L. Perera and F. G. Amar, *J. Chem. Phys.* **90**, 7354 (1989).
- I. Benjamin, U. Banin, and S. Ruhman, *J. Chem. Phys.* **98**, 8337 (1993).
- I. Benjamin and R. M. Whitnell, *Chem. Phys. Lett.* **204**, 45 (1993).
- J. T. Hynes, H. J. Kim, J. R. Mathis, R. Bianco, K. Ando, and B. J. Gertner, in *Reaction Dynamics in Clusters and Condensed Phases*, edited by B. Pullman and J. Jortner (Kluwer Academic, Dordrecht, 1994), p. 289.
- B. J. Gertner, K. Ando, R. Bianco, and J. T. Hynes, *Chem. Phys.* **183**, 309 (1994).
- J. M. Papanikolas, Ph.D. thesis, 1994.
- E. C. M. Chen and W. E. Wentworth, *J. Phys. Chem.* **89**, 4099 (1985).
- MOLPRO, a package of *ab-initio* programs written by H.-J. Werner and P. J. Knowles with contributions from J. Almlöf, R. Amos, S. Elbert, K. Hampel, W. Meyer, K. Peterson, R. Pitzer, and A. Stone, version 92.7 (1992).
- H.-J. Werner and P. J. Knowles, *J. Chem. Phys.* **89**, 5803 (1988).
- P. J. Knowles and H.-J. Werner, *Chem. Phys. Lett.* **145**, 514 (1988).
- M. Dolg, Ph.D. thesis, 1989.

- ²³ P. W. Atkins, *Molecular Quantum Mechanics* (Oxford U.P., Oxford, 1983).
- ²⁴ R. S. Mulliken, *J. Chem. Phys.* **7**, 14, 20 (1939).
- ²⁵ Perera and Amar¹² note that the negative charge is not strongly bound to the dihalide ion, so it is expected to be strongly perturbed by the CO_2 molecules (p. 7367). The charge switching function should depend upon the solvent configuration, whereas in their model it is only a function of the dihalide bond length.
- ²⁶ C. S. Murthy, K. Singer, M. L. Klein, and I. R. McDonald, *Mol. Phys.* **40**, 1517 (1980 and references contained therein).
- ²⁷ V. W. Maslen and C. A. Coulson, *J. Chem. Soc.* 4041 (1957).
- ²⁸ To our knowledge the only published *ab initio* results for I_2^- are the valence bond calculations of Tasker *et al.* which used large core potentials and very small basis sets, P. W. Tasker, G. G. Balint-Kurti, and R. N. Dixon, *Mol. Phys.* **32**, 1651 (1976).
- ²⁹ Perera and Amar¹² approximated the polarizability of Br_2^- by that of two (neutral) bromine atoms. Such a model fails to predict that the charge localizes on one nucleus when an electric field is applied.
- ³⁰ A. Szabo and N. S. Ostlund, *Modern Theoretical Chemistry* (MacMillan, London, 1982).
- ³¹ Y. N. Demkov, *Zh. Eksp. Teor. Fiz.* **45**, 195 (1963).
- ³² Y. N. Demkov, *Sov. Phys. JETP* **18**, 138 (1964).
- ³³ J. H. Van Vleck, *Phys. Rev.* **33**, 467 (1929).
- ³⁴ D. W. Arnold, S. E. Bradforth, E. H. Kim, and D. M. Neumark, *J. Chem. Phys.* **97**, 9468 (1992).
- ³⁵ H. J. Kim and J. T. Hynes, *J. Chem. Phys.* **96**, 5088 (1992).
- ³⁶ G. Herzberg, *Molecular Spectra and Molecular Structure III. Electronic Spectra and Electronic Structure of Polyatomic Molecules* (Krieger, Malabar, FL, 1991).
- ³⁷ J. C. Tully, *J. Chem. Phys.* **58**, 1396 (1973).
- ³⁸ J. C. Tully, *J. Chem. Phys.* **59**, 5122 (1973).
- ³⁹ G. Herzberg, *Molecular Spectra and Molecular Structure I. Spectra of Diatomic Molecules* (Van Nostrand Reinhold, New York, 1950).
- ⁴⁰ E. P. Wigner and E. E. Witmer, *Z. Physik* **51**, 859 (1928).
- ⁴¹ H. A. Kramers, *Koninkl. Ned. Akad. Wet. Proc.* **33**, 959 (1930).
- ⁴² E. P. Wigner, *Group Theory and Its Application to the Quantum Mechanics of Atomic Spectra*, translated by J. J. Griffin (Academic, New York, 1959).
- ⁴³ A. W. Joshi, *Elements of Group Theory for Physicists* (Wiley, New York, 1973).
- ⁴⁴ R. N. Zare, *Angular Momentum, Understanding Spatial Aspects in Chemistry and Physics* (Wiley, New York, 1988), p. 78.
- ⁴⁵ R. N. Zare, *Angular Momentum, Understanding Spatial Aspects in Chemistry and Physics* (Wiley, New York, 1988), p. 89 and Eqs. (3.52), (3.54) and (3.103).
- ⁴⁶ E. U. Condon and G. H. Shortley, *The Theory of Atomic Spectra* (Cambridge U.P., Cambridge, 1951), p. 48.
- ⁴⁷ E. U. Condon and G. H. Shortley, *The Theory of Atomic Spectra* (Cambridge U.P., Cambridge 1951), p. 123 Eqs. (8a) and (8b), and p. 66.
- ⁴⁸ H. Lefebvre-Brion and R. W. Field, *Perturbations in the Spectra of Diatomic Molecules* (Academic, New York, 1986).
- ⁴⁹ S. Wolfram, *Mathematica*, version 2 (Wolfram Research Inc., Champaign, IL, 1988).
- ⁵⁰ J. C. Tully, *J. Chem. Phys.* **93**, 1061 (1990).
- ⁵¹ J. Faeder, R. Parson, and P. E. Maslen, work in progress (1994).
- ⁵² N. F. Mott, *Proc. Cambridge Philos. Soc.* **27**, 553 (1931).
- ⁵³ G. Parlant and M. H. Alexander, *J. Chem. Phys.* **92**, 2287 (1990).
- ⁵⁴ J. C. Tully and R. K. Preston, *J. Chem. Phys.* **55**, 562 (1971).
- ⁵⁵ M. Karplus, R. N. Porter, and R. D. Sharma, *J. Chem. Phys.* **43**, 3259 (1965).
- ⁵⁶ D. W. Jepsen and J. O. Hirschfelder, *J. Chem. Phys.* **32**, 1323 (1960).
- ⁵⁷ W. R. Thorson, *J. Chem. Phys.* **42**, 3878 (1965).
- ⁵⁸ H. S. W. Massey, *Rep. Progr. Phys.* **12**, 248 (1949).
- ⁵⁹ This analysis breaks down if the solvation effects are very strong, because extra configurations (especially I^*-I^-) are mixed into the ${}^2\Pi_{g,1/2}$ wave function. The potential energy surface and charge switching function are displayed in Figs. 1(c), 1(d), and Fig. 3.
- ⁶⁰ D. H. Burde and R. A. McFarlane, *J. Chem. Phys.* **64**, 1850 (1976).
- ⁶¹ If the $I_2^- \cdots CO_2$ collision is collinear then 1/2 \rightarrow 3/2 transitions are forbidden in the classical path approximation. This can be seen by classifying the wave functions and the operator d/dR corresponding to the reaction coordinate in the C_{2v} point group. The operator is totally symmetric whereas the wave functions are of different symmetry (Table I), so the transition matrix element $\langle 1/2|d/dR|3/2\rangle$ will be zero.